Report No. 77-7

PURDUE UNIVERSITY
SCHOOL OF AERONAUTICS AND ASTRONAUTICS

EFFECTS OF DYNAMIC AEROELASTICITY ON HANDLING QUALITIES AND PILOT RATING

Wen-Yo Yen and Robert L. Swaim

December 1977

West Lafayette, Indiana 47907

Report No. 77-7

PURDUE UNIVERSITY

SCHOOL OF AERONAUTICS AND ASTRONAUTICS

EFFECTS OF DYNAMIC AEROELASTICITY ON HANDLING QUALITIES AND PILOT RATING

Wen-Yo Yen and Robert L. Swaim

December 1977

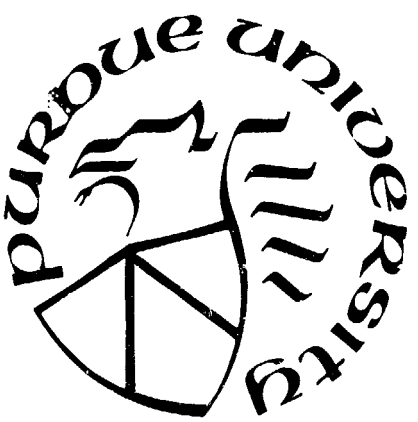

West Lafayette, Indiana 47907

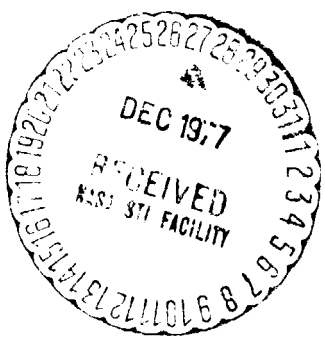

ACKNOWLEDGEMENTS

First and foremost, I would like to thank my advisor, Dr. Robert L. Swaim, for his technical guidance, suggestions, and patience throughout this study. Appreciation is also extended to the members of my advisory committee:

Prof. D.W. Alspaugh

Prof. Hsu Lo

Prof. C.L. Nachtigal

for their consultation in this effort. In addition, I would like to thank Dr. William Seitz and Dr. James Silverthorn who originally constructed the simulator for their own thesis work.

This research was supported in part by the Vehicle Dynamics and Control Division of the NASA Dryden Flight Research Center under grant NSG 4003. Mr. Donald T. Berry, Technical Monitor.

TABLE OF CONTENTS

	Page
LIST OF TABLES	v
LIST OF FIGURES	vii
LIST OF SYMBOLS	ix
ABSTRACT	xiii
CHAPTER 1 - INTRODUCTION	1
1.1 Handling Qualities and Pilot Rating	1
1.2 Handling Quality History	2
1.3 Objectives	4
1.4 Thesis Organization	5
CHAPTER 2 - EQUATIONS OF MOTION	6
2.1 General Description of the Aircraft	6
2.2 Airframe Equations	6
2.3 Flight Director Equation	21
2.4 Pitch Angle Error Equation	23
2.5 Summary Equations	26
CHAPTER 3 - DYNAMIC CHARACTERISTICS OF EIGHT CASES	28
3.1 General Description	28
3.2 Dynamic Characteristics of Case 1, Case 2, and Case 3	28
3.3 Dynamic Characteristics of Case 4	30
3.4 Dynamic Characteristics of Case 5 and Case 6	35
3.5 Dynamic Characteristics of Case 7 and Case 8	35
3.6 Summary of Eight Cases	41
CHAPTER 4 - EXPERIMENT	46
4.1 Overview	46
4.2 Apparatus	47
4.3 Methodology	50

Page

CHAPTER 5 - RESULTS 55

5.1 Method of Analysis 55
5.2 Comparison of Cases 60
5.3 Time Histories 69

CHAPTER 6 - SUMMARY 89

6.1 Summary 89
6.2 Conclusions 90
6.3 A Recommendation 91

BIBLIOGRAPHY 93

APPENDIX - ANALOG SIMULATION 95

LIST OF TABLES

Table		Page
2.1	Force and Moment and Elastic Force Derivatives as a Function of Stability Derivatives	18
2.2	Stability Derivatives for B-1 Bomber in Mach 0.85 Flight Condition	20
2.3	Equations of Motion in Matrix Form	27
3.1	Dynamic Characteristics of Case 1	31
3.2	Dynamic Characteristics of Case 2	32
3.3	Dynamic Characteristics of Case 3	33
3.4	Dynamic Characteristics of Case 4	36
3.5	Dynamic Characteristics of Case 5	38
3.6	Dynamic Characteristics of Case 6	39
3.7	Dynamic Characteristics of Case 7	42
3.8	Dynamic Characteristics of Case 8	43
3.9	Natural Frequencies and Damping Ratios of Eight Cases	45
4.1	Order of Presentation of Cases	50
5.1	64 Observations of RMS Pitch Angle Error	57
5.2	Analysis of Variance	58
5.3	Summary of Results	62
5.4	Required Difference in Means for Statistical Significance	63

Table Page

5.5 Summary of Tracking Error, Cooper-Harper Rating, and Pilots' Comments 70

Appendix Table

A.1 Normalization of Variables 96

A.2 Potentiometer Settings 105

A.3 Potentiometer Settings for Eight Cases ... 107

LIST OF FIGURES

Figure		Page
2.1	B-1 Bomber and Sign Convention for Body Axes	7
2.2	Rigid and Elastic Pitch Angles	23
2.3a	Electronic Attitude-Director Display (EADI).	25
2.3b	The Airplane Attitude Corresponding to EADI Above	25
3.1	The Locus of Roots of Matrix A, Case 1, Case 2, Case 3, as a Function of Natural Frequency of Elastic Mode 1, ω_1	29
3.2	The Locus of Roots of Matrix A, Case 4, as a Function of Natural Frequency of Elastic Mode 2, ω_2	34
3.3	The Locus of Roots of Matrix A, Case 5, Case 6, as a Function of Natural Frequencies of Elastic Mode 1, ω_1, and Elastic Mode 2, ω_2	37
3.4	The Locus of Roots of Matrix A, Case 7, Case 8, as a Function of Natural Frequencies of Elastic Mode 1, ω_1, and Elastic Mode 2, ω_2	40
4.1	Block Diagram of Apparatus	48
4.2	Command Signal	52
5.1	Tracking Performance Versus Cases	61
5.2	Cooper-Harper Ratings	64
5.3	Sample Time History - Case 1	71
5.4	Sample Time History - Case 2	74
5.5	Sample Time History - Case 3	76

Figure		Page
5.6	Sample Time History - Case 4	78
5.7	Sample Time History - Case 5	80
5.8	Sample Time History - Case 6	83
5.9	Sample Time History - Case 7	85
5.10	Sample Time History - Case 8	87

Appendix Figure		
A.1	Z-Force Equation	97
A.2	Pitching Moment Equation	98
A.3	Structural Mode 1 Equation	99
A.4	Structural Mode 2 Equation	100
A.5	X-Force Equation and Altitude Equation ...	101
A.6	Pitch Command Input	102
A.7	Flight Director Equation and Pitch Angle Error Equation	103
A.8	Control Inputs	104

I_x, I_y, I_z	Stability axes mass moments of inertia
J_{xz}, J_{yz}, J_{xy}	Stability axes mass cross moments of inertia
L,M,N,	Roll, pitch, and yaw moments about the stability axes
L_i, M_i, N_i	Partial derivatives of x,y,z components of aerodynamic moments with respect to variable "i"
m	Aircraft mass
P_1, P_2, P_3, P_4	Pilots (subjects for experiment)
P,Q,R	Total roll, pitch, and yaw rates about the stability axes
p,q,r	Perturbation roll, pitch, and yaw rates about the stability axes
Q_{η_i}	Generalized force in ith elastic mode
$Q_{\eta i_j}$	Partial derivative of generalized force of ith elastic mode with respect to variable "j"
RMS	Root mean square
S	Aircraft wing reference area
SD	Standard deviation
T,t	Time
U,V,W	Components of $\bar{V}$
u,v,w	Components of perturbation linear velocity
u	Control variable
$\bar{V}$	Total linear velocity vector
X_i, Y_i, Z_i	Partial derivative of x,y,z components of aerodynamic forces with respect to variable "i"
x	Vector of state variables

Greek

α	Angle of attack (rad)
γ	Flight path angle - angle between velocity vector and horizontal
δ_a	Incremental aileron deflection - positive for right roll (rad)
δ_r	Incremental rudder deflection - positive for left turn (rad)
δ_e	Incremental elevator deflection - positive for nose pitch down (rad)
δ_t	Incremental thrust variation - positive for increase in thrust (pounds)
δ_f	Incremental flap deflection - positive for less flap deflection (rad)
ζ_i	Structural damping ratio, mode i
ζ_{ie}	Coupled damping ratio of ith mode
η_i	Generalized displacement of the ith normalized structural mode
ρ	Air density (slugs/ft^3)
Ψ,Θ,Φ	Heading, pitch and roll angles
ψ,θ,ϕ	Perturbation heading, pitch and roll angles
$\phi_i()$	The ith normalized mode shape, i.e., ratio of local deflection to that at normalizing point (nondimensional); () denotes location on fuselage centerline
$\phi_i'()$	Slope of the ith normalized mode; () denotes location
$\sum(\cdot)$	Summation operator
$\bar{\omega}$	Angular velocity vector

ω_i	Undamped natural frequency of ith mode
ω_{ie}	Coupled undamped natural frequency of ith mode

Subscripts

A	Vector written in aircraft coordinates
c	Flight director pitch command
I	Vector written in inertial coordinates
o	Trimmed value about which perturbation variables obtained
ph	Phugoid
SP	Short period
T	Matrix transpose
1,2,3	Intermediate coordinate systems used to obtain Euler angles

ABSTRACT

Yen, Wen-Yo. Ph.D., Purdue University, December 1977. Effects of Dynamic Aeroelasticity on Handling Qualities and Pilot Rating. Major Professor: Robert L. Swaim.

Pilot performance parameters, such as pilot ratings, tracking errors, and pilot comments were determined for a longitudinal pitch tracking task using a large, flexible bomber with parametric variations in the undamped natural frequencies of the two lowest frequency symmetric elastic modes. This pitch tracking task was programmed on a fixed base simulator with an electronic attitude-director display of pitch command, pitch angle, and pitch error. The results of this study indicate that low-frequency structural flexibility can significantly affect the handling qualities and pilot ratings in the task evaluated.

CHAPTER 1

INTRODUCTION

1.1 Handling Qualities and Pilot Rating

The way an airplane in flight responds to control inputs by the pilot is referred to as the handling qualities of the vehicle. If the handling qualities are not good, the pilot must devote more of his attention to flying the airplane and less to other mission activities, such as weapon delivery and air-to-air combat. In other words, the worse the airplane handles, the greater the pilot workload. In simple terms, handling qualities relate to the ease or difficulty in attempting to maneuver or control an aircraft. The study of handling qualities is 100% pilot oriented.

Although all the individual factors contributing to handling qualities may fall in the satisfactory or acceptable ranges of their respective boundaries, their composite effect may still not produce a completely satisfactory airplane in some cases. Proof of the total system handling qualities is usually required by ground-based simulation and/or flight test of the actual airplane. A tool that is widely used in such evaluations is the Cooper-Harper

Pilot Opinion Rating Scale (reference 8). It is a ten-point numerical scale whereby the pilot can express his evaluation or opinion of how well the airplane flys or handles.

1.2 Handling Qualities History

There were only a few attempts to design an aircraft for good handling qualities before the second world war era. Before then the design of aircraft concentrated primarily on aircraft performance goals. Stability and control characteristics were not well understood. It was known, however, that static and dynamic stability characteristics and control system design determined the handling qualities - good or bad - of an aircraft. However, since that era much has been done to analyze the handling qualities of existing aircraft and to develop theories that allow the stability and control engineers to design an aircraft that handles well.

Presently, designers mainly consider the rigid aircraft to estimate the handling qualities and pilot rating of the airplane. But large airplanes such as transport category airplanes and bombers need to be as light as possible due to many reasons which include fuel conservation. This means a sacrifice in structural rigidity. Airplane flexure causes additional aerodynamic loads which in turn cause additional flexure, etc. Also coupling occurs between the elastic modes and the rigid body motion

as the gyros sense the flexure motion and the rigid body motion.

To point out the near complete lack of knowledge as to how dynamic aeroelastic modes affect airplane handling qualities, we quote the only reference to their effects contained in MIL-F-8785B, Military Specification - Flying Qualities of Piloted Airplanes (reference 2). The four-line statement merely says: "Since aeroelasticity, control equipment, and structural dynamics may exert an important influence on the airplane flying qualities, such effects should not be overlooked in calculations or analyses directed toward investigation of compliance with the requirements of this specification." The specification is concerned only with desirable ranges of values on rigid-body dynamic response parameters. It seems quite possible that the handling qualities and pilot rating could be significantly affected by elastic modes, particularly in case some modes have low natural frequencies. It is not at all clear that the handling qualities should be specified by rigid-body dynamic parameters when such rigid and elastic mode interaction is present. The pilot will likely not be able to discern, for example, how much of a given pitch angle response to command input is due to rigid-body and how much is due to low frequency elastic modes. These interactions certainly affected the pilot's assessment of the handling qualities in the work reported herein.

Therefore, some study of these elastic effects and revised design standards must be inaugurated for large flexible vehicles. To date no design criteria exist for handling qualities in terms of control system specifications. It is hoped that this thesis will be a basic step in that direction.

1.3 Objectives

The longitudinal dynamics of the Rockwell B-1 bomber aircraft was simulated on an analog computer. The two lowest frequency symmetric elastic modes were included in the math model. This was sufficient to get an appreciation for the effects on pilot rating, where the elastic mode characteristics were varied between runs.

A fixed base, pilot in the loop simulation was performed to examine the handling qualities and pilot ratings with variations in each of the undamped natural frequencies of the two elastic modes. Specifically, the following questions were addressed:

1. What are the relative pilot ratings in a pitch tracking task as a function of lowering elastic mode frequencies?
2. Which frequency combinations produce the poorest pilot performance?
3. Which of these two elastic modes has the most significant effects on the handling qualities and pilot rating?

Pilot pitch tracking performance, Cooper-Harper rating, and pilot comments were used to answer these questions.

1.4 Thesis Organization

Chapter 2 mathematically establishes the task. The aircraft dynamic equations are derived and the simplifications implicit in the perturbation technique and aeroelastic effects are discussed. In addition, a flight director equation and a pitch angle error equation, including their functions in this study, are presented.

Chapter 3 discusses how and why the eight cases are chosen for this study. The dynamic characteristics of eight cases are presented.

Chapter 4 discusses the experimental objectives, apparatus, and methodology for the fixed base, pilot in the loop simulation.

Chapter 5 gives the results of this simulation study. The eight cases are compared and the difficulty of some cases is discussed.

Chapter 6 concludes the thesis by reviewing the results, outlining areas that require additional study, and recommending further activities.

CHAPTER 2

EQUATIONS OF MOTION

2.1 General Description of the Aircraft

The aircraft simulated in this study is the B-1 bomber, an American built, large flexible aircraft (Figure 2.1). Rockwell International examined this aircraft which they designed (reference 3) and found they were able to fly a sea level zero degree trim pitch angle at 562.2 knots (949 feet per second airspeed) with the elevators up 6 degrees. It is from these studies that much of the aircraft data (mass, stability derivatives, etc.) was obtained.

There is a reason the B-1 bomber was used in our studies. This airplane is large and flexible enough to exhibit the desired effects between fuselage elastic motion and rigid-body motion.

2.2 Airframe Equations

In order to write equations of motion one must first establish a coordinate system. It is common practice to attach a body-fixed coordinate system to the aircraft and write equations with respect to it. By doing so all moments of inertia will remain constant. The stability

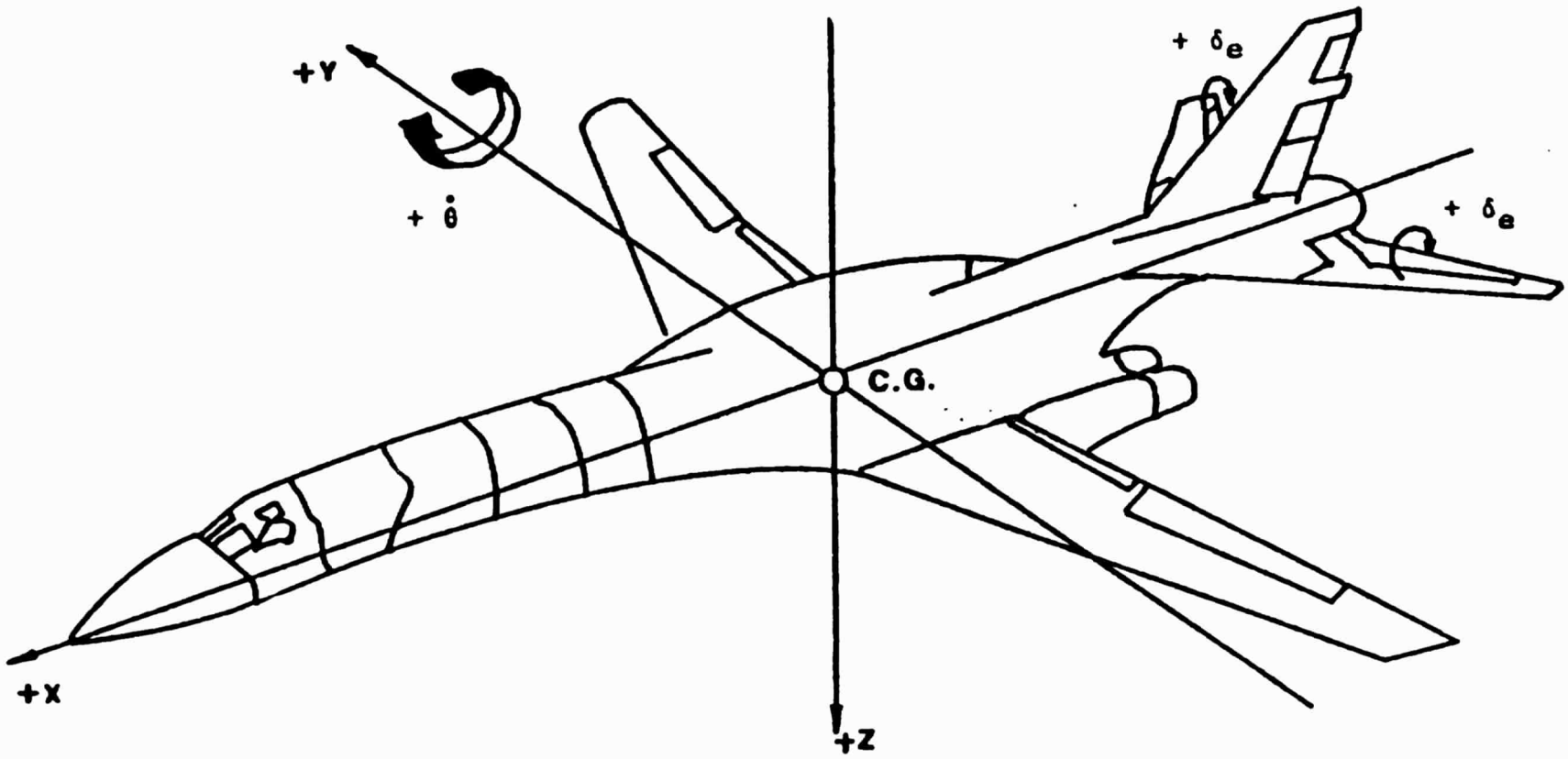

Figure 2.1 B-1 Bomber and Sign Convention for Body Axes

axes convention is to let the X axis point forward, the Y axis point out the right wing, and the Z axis point downward.

I. Rigid Body Equations

Assuming constant mass:

$$\bar{F} = m\frac{d\bar{v}}{dt}\Big|_I = m\left(\frac{d\bar{v}}{dt}\Big|_B + \bar{\omega} \times \bar{V}\right) \tag{2.1}$$

$$\bar{M} = \frac{d\bar{H}}{dt}\Big|_I = \frac{d\bar{H}}{dt}\Big|_B + \bar{\omega} \times \bar{H} \tag{2.2}$$

where:

$\frac{d\bar{v}}{dt}\Big|_I$ is the rate of change of the aircraft velocity vector as seen from inertia coordinates.

$\frac{d\bar{v}}{dt}\Big|_B$ is the rate of change as seen from aircraft body axes.

$\bar{\omega}$ is the angular velocity of the aircraft.

$\bar{H}$ is the aircraft angular momentum vector.

$\bar{F}$ is the vector sum of all external forces.

$\bar{M}$ is the vector sum of all external moments.

m is the aircraft mass.

These two vector equations can be written in terms of their components to produce the following six equations:

$$G_x + F_x = m(\dot{U} + QW - RV) \tag{2.3}$$

$$G_y + F_y = m(\dot{V} + RU - PW) \tag{2.4}$$

$$G_z + F_z = m(\dot{W} + PV - QU) \tag{2.5}$$

$$L = \dot{P}I_x - \dot{R}J_{xz} + QR(I_z - I_y) - PQJ_{xz} \tag{2.6}$$

$$M = \dot{Q}I_y + RP(I_x - I_z) + (P^2 - R^2)J_{xz} \tag{2.7}$$

$$N = \dot{R}I_z - \dot{P}J_{xz} + PQ(I_y - I_x) + QRJ_{xz} \tag{2.8}$$

where, in body coordinates:

U, V, W are the components of $\bar{V}$

P, Q, R are the components of $\bar{\omega}$

G_x, G_y, G_z are the components of the gravity forces

F_x, F_y, F_z are the components of the aerodynamic forces

L, M, N are the components of the external moments

I_x, I_y, I_z are the mass momen s of inertia

J_{xz} is the cross moment of inertia (J_{xy} and J_{zy} are zero because the X-Z plane is a plane of symmetry).

This body axis frame can be referenced to an inertial coordinate system by a translation of the center of mass and three rotations. Using the subscript "I" to identify the inertial coordinate system, "3" the instantaneous

body axes coordinate system, and "1" and "2" intermediate coordinate systems, the transformation takes place in the following order:

(1) starting with the "I" coordinate system, rotate about z_I through an angle Ψ to establish a new coordinate system x_1, y_1, z_1.

(2) Then rotate about y_1 through an angle Θ to establish a new coordinate system x_2, y_2, z_2.

(3) Finally, rotate about x_2 through an angle Φ to get to the aircraft fixed coordinate system x_3, y_3, z_3.

From this description one can see that $\dot{\Phi}$, $\dot{\Theta}$, $\dot{\Psi}$ point along x_3, y_2, z_1 respectively, whereas P, Q, R lie along x_3, y_3, z_3. They are related by the equations:

$$\begin{aligned} P &= \dot{\Phi} - \dot{\Psi} \sin \Theta \\ Q &= \dot{\Theta} \cos \Phi + \dot{\Psi} \cos \Theta \sin \Phi \\ R &= \dot{\Psi} \cos \Theta \cos \Phi - \dot{\Theta} \sin \Phi \end{aligned} \tag{2.9}$$

The external forces and moments come from two sources: gravity and aerodynamic forces. Gravity, because it acts through the center of mass, produces no external moments. It does produce an external force that decomposes into:

$$\begin{aligned} G_x &= - mg \sin \Theta \\ G_y &= + mg \cos \Theta \sin \Phi \\ G_z &= + mg \cos \Theta \cos \Phi \end{aligned} \tag{2.10}$$

along the x_3, y_3, z_3 axes, respectively.

Up to this point very few assumptions have been made and as a result the equations are all nonlinear. By assuming that the aircraft will only make small perturbations from some steady state condition (a reasonable assumption for a longitudinal tracking task) the equations can be greatly simplified.

Let:

$$U = U_0 + u \qquad P = P_0 + p \qquad \Theta = \Theta_0 + \theta$$

$$V = V_0 + v \qquad Q = Q_0 + q \qquad \Phi = \Phi_0 + \phi \tag{2.11}$$

$$W = W_0 + w \qquad R = R_0 + r \qquad \Psi = \Psi_0 + \psi$$

Where the "0" subscript refers to the trimmed value and the small letters are the perturbation variables. The following trimmed condition was chosen:

$$U_0 = 949 \text{ ft/sec}$$

$$\theta_0 = 0 \text{ degree} \tag{2.12}$$

$$\alpha_0 = 3 \text{ degrees}$$

$$V_0 = W_0 = P_0 = Q_0 = R_0 = \Phi_0 = \Psi_0 = 0$$

The steady state control settings for this flight condition turn out to be:

Throttle = 41,712 pounds thrust

Elevator = - 6 degrees (2.13)

and all other controls trimmed out to zero. The incremental control variables are represented by δ_e, δ_t for

elevator and thrust. They represent changes from the above trimmed value.

This same linearization technique can be applied to the aerodynamic forces and moments. This is done by separating them into a steady state term and linear terms due to the perturbation variables. For example:

$$F_x = F_{x_0} + \left.\frac{\partial F_x}{\partial u}\right|_0 u + \left.\frac{\partial F_x}{\partial \alpha}\right|_0 \alpha + \left.\frac{\partial F_x}{\partial \dot{\alpha}}\right|_0 \dot{\alpha} + \left.\frac{\partial F_x}{\partial \dot{\theta}}\right|_0 \dot{\theta} + \left.\frac{\partial F_x}{\partial \delta_e}\right|_0 \delta e \qquad (2.14)$$

where $\alpha = \frac{w}{U_o}$ $\qquad \dot{\theta} = q$.

The same is done for F_y, F_z, L, M, and N.

The partial derivatives are a function of the characteristics of the aircraft and the particular trimmed condition at which they are evaluated. For the trimmed condition selected, F_x, F_z, and M are independent of v, p, r, ψ, ϕ, δ_a, δ_r while F_y, L, N are independent of u, w, q, θ, δ_e, δ_t, δ_f. As a result, all the corresponding partial derivatives are zero.

Combining equations 2.3 - 2.14, expanding the trigonometric functions, and neglecting all second order terms (such as "qw" or "rv"), results in the following nine equations:

$$p = \dot{\phi} - \dot{\psi} \sin \Theta_0$$

$$q = \dot{\theta}$$

$$r = \dot{\psi} \cos \Theta_0 \qquad (2.15)$$

$$m\dot{u} = -mg\theta\cos\Theta_0+X_u u+X_\alpha\alpha+X_q q+X_{\delta_e}\delta e+X_{\delta_t}\delta t+X_{\delta_f}\delta f$$

$$m(\dot{v}+U_0 r)=mg\phi\cos\Theta_0+Y_v v+Y_p p+Y_r r+Y_{\delta_a}\delta a+Y_{\delta_r}\delta r$$

$$m(\dot{w}-U_0 q)=-mg\theta\sin\Theta_0+Z_u u+Z_\alpha\alpha+Z_{\dot{\alpha}}\dot{\alpha}+Z_q q+Z_{\delta_e}\delta e+Z_{\delta_t}\delta t+Z_{\delta_f}\delta f$$

$$\dot{p}I_x-\dot{r}J_{xz}=L_v v+L_p p+L_r r+L_{\delta_a}\delta a+L_{\delta_r}\delta r$$

$$\dot{q}I_y=M_u u+M_\alpha\alpha+M_{\dot{\alpha}}\dot{\alpha}+M_q q+M_{\delta_e}\delta e+M_{\delta_t}\delta t+M_{\delta_f}\delta f$$

$$\dot{r}I_z-\dot{p}J_{xz}=N_v v+N_p p+N_r r+N_{\delta_a}\delta a+N_{\delta_r}\delta r$$

This aircraft is considered to be in straight and level unaccelerated flight and then to be disturbed by deflection of the elevator. This deflection applies a pitching moment causing a rotation which eventually causes a change in F_x and F_z, but does not cause a rolling or yawing moment or any change in F_y; thus P=R=V=0 and the equations 2.4, 2.6, 2.8, may be eliminated, resulting in the following equations:

$$q=\dot{\theta}$$

$$m\dot{u}=-mg\theta+X_u u+X_\alpha\alpha+X_{\delta_e}\delta e+X_{\delta_t}\delta t$$

$$U_0 m\dot{\alpha}=mU_0\dot{\theta}+Z_u u+Z_\alpha\alpha+Z_{\dot{\alpha}}\dot{\alpha}+Z_{\dot{\theta}}\dot{\theta}+Z_{\delta_e}\delta e \qquad (2.16)$$

$$I_y\ddot{\theta}=M_u u+M_\alpha\alpha+M_{\dot{\alpha}}\dot{\alpha}+M_{\dot{\theta}}\dot{\theta}+M_{\delta e}\delta e$$

where X_f, Z_{δ_t}, Z_{δ_f}, M_{δ_t}, and M_{δ_f} are assumed zero, and $\Theta_0=0$.

II. Elastic Mode Equations

The most common method of accounting for the dynamic aeroelastic effects is to represent the deflection of the aircraft in terms of its normal modes of free vibration. The instantaneous deflection of any point on the structure, from the rigid steady-state condition as measured in the body axes frame, can be expressed as a vector sum of deflection components in the X, Y, and Z directions. Deflection in the Z direction and perpendicular to the XY plane is indicated by $\xi_z(x, y, t)$, where the planform has been idealized to a flat plate in the XY plane. Deflection in the Y direction and perpendicular to the XZ plane is $\xi_y(x, z, t)$, where the side view planform has been idealized to a plate in the XZ plane. Deflection in the X direction has a negligible effect on dynamic stability and is neglected.

For longitudinal equations of motion we only need to consider the deflection in the Z direction which is $\xi_z(x, y, t)$. The instantaneous deflections can be represented as a sum of an infinite number of orthogonal normal vibration modes as follows:

$$\xi_z(x,y,t) = \sum_{i=1}^{\infty} \phi_i(x,y)\eta_i(t) \qquad (2.17)$$

where:

$\phi_i(x,y)$ is the ith symmetric normalized mode shape in the XY plane.

$\eta_i(t)$ is the generalized displacement.

Representation of vibration in terms of normal modes results in additional equations of motion of the form (reference 1).

$$m_i[\ddot{\eta}_i + 2\zeta_i \omega_i \dot{\eta}_i + \omega_i^2 \eta_i] = Q_{\eta_i}(t) \qquad (2.18)$$

m_i is generalized mass defined by

$$m_i = \iint m(x,y)\phi_i^2(x,y)\,dxdy$$

where:

$m(x,y)$ is the structural mass density per unit area in the respective XY idealized planform.

$Q_{\eta_i}(t)$ is the generalized force defined by

$$Q_{\eta_i}(t) = \iint f_z(x,y,t)\phi_i(x,y)\,dxdy$$

where:

$f_z(x,y,t)$ is the time-dependent aerodynamic pressure distribution acting in the Z direction.

η_i is an additional dependent variable to be introduced into the rigid-body equations as well as appearing in (2.18). Considering the longitudinal rigid-body equations (2.16), they will contain additional

aerodynamic terms due to aeroelasticity as follows:

$$\sum_{i=1}^{\infty} \left[\frac{\partial Z}{\partial \eta_i} \eta_i + \frac{\partial Z}{\partial \dot{\eta}_i} \dot{\eta}_i \right]$$

$$\sum_{i=1}^{\infty} \left[\frac{\partial M}{\partial \eta_i} \eta_i + \frac{\partial M}{\partial \dot{\eta}_i} \dot{\eta}_i \right] \qquad (2.19)$$

In order to make the elastic equations (2.18) compatible with the rigid-body equations, the $Q_{\eta_i}(t)$ must be expressed in terms of the dependent variables. Thus:

$$Q_{\eta_i}(t) = \frac{\partial Q_{\eta_i}}{\partial \alpha} \alpha + \frac{\partial Q_{\eta_i}}{\partial q} q + \frac{\partial Q_{\eta_i}}{\partial \delta_e} \delta_e + \frac{\partial Q_{\eta i}}{\partial \dot{\alpha}} \dot{\alpha}$$

$$+ \sum_{k=1}^{\infty} \frac{\partial Q_{\eta_i}}{\partial \eta_k} \eta_k + \sum_{k=1}^{\infty} \frac{\partial Q_{\eta i}}{\partial \dot{\eta}_k} \dot{\eta}_k \qquad (2.20)$$

The numerous partial derivatives are obtained by utilizing the stability derivatives of the aircraft. Listed in Table 2.1 is the relationship between these partial derivatives and the stability derivatives while Table 2.2 gives the values of these derivatives for the B-1 bomber at the Mach 0.85, sea level flight condition.

Using Tables 2.1 and 2.2 to evaluate the coefficients in equations 2.16 and 2.18 results in the following equations,

$$\dot{u} = -0.025u-25.0\alpha-32.2\theta+0.000141\delta_t$$

$$\dot{\alpha} = -0.00065u-1.205\alpha+0.943\dot{\theta}-0.00905\eta_1-0.00021\dot{\eta}_1 +0.00465\eta_2+0.00015\dot{\eta}_2-0.2888\delta_e$$

$$\ddot{\theta} = -0.0026u-7.649\alpha-0.481\dot{\alpha}-1.566\dot{\theta}-0.1889\eta_1-0.00754\dot{\eta}_1 +0.210\eta_2+0.00704\dot{\eta}_2-15.193\delta_e \qquad (2.21)$$

$$\ddot{\eta}_1+0.272\dot{\eta}_1+184.69\eta_1=-735.19\alpha+2.264\dot{\alpha}-135.404\dot{\theta}+7.263\eta_1 -0.866\dot{\eta}_1-15.889\eta_2+0.915\dot{\eta}_2-2228.4\delta_e$$

$$\ddot{\eta}_2+0.424\dot{\eta}_2+448.59\eta_2=764.70\alpha+6.153\dot{\alpha}+50.149\dot{\theta}+7.041\eta_1 -0.1206\dot{\eta}_1-7.962\eta_2-0.426\dot{\eta}_2+614.96\delta_e$$

Additional details of the derivation of perturbation equations for an aircraft simulation are presented in references 6, 7, 14.

Table 2.1 Force and Moment and Elastic Force Derivatives as a Function of Stability Derivatives

$a_1 = \rho U_0^2 S/2$

$a_2 = a_1 c/2U_0$

$X_u = a_1 C_{x_u}/U_0$	$Z_u = a_1 C_{z_u}/U_0$	$M_u = a_1 c C_{m_u}/U_0$
$X_\alpha = a_1 C_{x_\alpha}$	$Z_\alpha = a_1 C_{z_\alpha}$	$M_\alpha = a_1 c C_{m_\alpha}$
$X_{\dot{\alpha}} = a_2 C_{x_{\dot{\alpha}}}$	$Z_{\dot{\alpha}} = a_2 C_{z_{\dot{\alpha}}}$	$M_{\dot{\alpha}} = a_2 c C_{m_{\dot{\alpha}}}$
$X_{\dot{\theta}} = a_2 C_{x_{\dot{\theta}}}$	$Z_{\dot{\theta}} = a_2 C_{z_{\dot{\theta}}}$	$M_{\dot{\theta}} = a_2 c C_{m_{\dot{\theta}}}$
$X_{\delta e} = a_1 C_{x_{\delta e}}$	$Z_{\delta e} = a_1 C_{z_{\delta e}}$	$M_{\delta e} = a_1 c C_{m_{\delta e}}$
$X_{\delta t} = 1^*$	$Z_{\delta t} = 0$	$M_{\delta t} = 0$
$X_{\eta_1} = a_1 C_{x_{\eta_1}}$	$Z_{\eta_1} = a_1 C_{z_{\eta_1}}$	$M_{\eta_1} = a_1 c C_{m_{\eta_1}} \eta_1$
$X_{\dot{\eta}_1} = a_1 C_{x_{\dot{\eta}_1}}/U_0$	$Z_{\dot{\eta}_1} = a_1 C_{z_{\dot{\eta}_1}}/U_0$	$M_{\dot{\eta}_1} = a_1 c C_{m_{\dot{\eta}_1}}/U_0$
$X_{\eta_2} = a_1 C_{x\eta_2}$	$Z_{\eta_2} = a_1 C_{z_{\eta_2}}$	$M_{\eta_2} = a_1 c C_{m_{\eta_2}}$
$X_{\dot{\eta}_2} = a_1 C_{x\dot{\eta}_2}/U_0$	$Z_{\dot{\eta}_2} = a_1 C_{z_{\dot{\eta}_2}}/U_0$	$M_{\dot{\eta}_2} = a_1 c C_{m_{\dot{\eta}_2}}/U_0$

*Obtained from reference 3.

Table 2.1, cont.

$Q_{\eta_{1_\alpha}} = a_1 C_{\eta_{1_\alpha}}$	$Q_{\eta_{2_\alpha}} = a_1 C_{\eta_{2_\alpha}}$
$Q_{\eta_{1_{\dot{\alpha}}}} = a_2 C_{\eta_{1_{\dot{\alpha}}}}$	$Q_{\eta_{2_{\dot{\alpha}}}} = a_2 C_{\eta_{2_{\dot{\alpha}}}}$
$Q_{\eta_{1_{\dot{\theta}}}} = a_2 C_{\eta_{1_{\dot{\theta}}}}$	$Q_{\eta_{2_{\dot{\theta}}}} = a_2 C_{\eta_{2_{\dot{\theta}}}}$
$Q_{\eta_{1_{\eta_1}}} = a_1 C_{\eta_{1_{\eta_1}}}$	$Q_{\eta_{2_{\eta_1}}} = a_1 C_{\eta_{2_{\eta_1}}}$
$Q_{\eta_{1_{\dot{\eta}_1}}} = a_1 C_{\eta_{1_{\dot{\eta}_1}}}/U_0$	$Q_{\eta_{2_{\dot{\eta}_1}}} = a_1 C_{\eta_{2_{\dot{\eta}_1}}}/U_0$
$Q_{\eta_{1_{\eta_2}}} = a_1 C_{\eta_{1_{\eta_2}}}$	$Q_{\eta_{2_{\eta_2}}} = a_1 C_{\eta_{2_{\eta_2}}}$
$Q_{\eta_{1_{\dot{\eta}_2}}} = a_1 C_{\eta_{1_{\dot{\eta}_2}}}/U_0$	$Q_{\eta_{2_{\dot{\eta}_2}}} = a_1 C_{\eta_{2_{\dot{\eta}_2}}}/U_0$
$Q_{\eta_{1_{\delta_e}}} = a_1 C_{\eta_{1_{\delta e}}}$	$Q_{\eta_{2_{\delta_e}}} = a_1 C_{\eta 2_{\delta_e}}$

*Obtained from reference 3.

Table 2.2 Stability Derivatives for B-1 Bomber in Mach 0.85 Flight Condition

$C_{x_u} = -0.08066$	$C_{z_u} = -1.9659$	$C_{m_u} = -0.4546$
$C_{x_\alpha} = -0.08500$	$C_{z_\alpha} = -3.9367$	$C_{m_\alpha} = -1.41052$
$C_{x_{\dot{\alpha}}} = 0$	$C_{z_{\dot{\alpha}}} = -5$	$C_{m_{\dot{\alpha}}} = -11.005$
$C_{x_{\dot{\theta}}} = 0$	$C_{z_{\dot{\theta}}} = 17.8558$	$C_{m_{\dot{\theta}}} = -35.7556$
$C_{x_{\delta_e}} = 0$	$C_{z_{\delta_e}} = -.9426$	$C_{m_{\delta_e}} = -2.799$
$C_{x_{\eta_1}} = 0$	$C_{z_{\eta_1}} = 0.02922$	$C_{m_{\eta_1}} = -0.0348$
$C_{x_{\dot{\eta}_1}} = 0$	$C_{z_{\dot{\eta}_1}} = 0.6592$	$C_{m_{\dot{\eta}_1}} = -1.32169$
$C_{x_{\eta_2}} = 0$	$C_{z_{\eta_2}} = -0.015$	$C_{m_{\eta_2}} = 0.0387$
$C_{x_{\dot{\eta}_2}} = 0$	$C_{z_{\dot{\eta}_2}} = -0.4733$	$C_{m_{\dot{\eta}_2}} = 1.233$

Table 2.2, cont.

$C_{n_{1_\alpha}} = -0.06478$	$C_{n_{2_\alpha}} = 0.48975$
$C_{n_{1_{\dot{\alpha}}}} = 0.02469$	$C_{n_{2_{\dot{\alpha}}}} = 0.48779$
$C_{n_{1_{\dot{\theta}}}} = -1.47658$	$C_{n_{2_{\dot{\theta}}}} = 3.97547$
$C_{n_{1_{n_1}}} = 0.00064$	$C_{n_{2_{n_1}}} = 0.00451$
$C_{n_{1\dot{n}_1}} = -0.07243$	$C_{n_{2\dot{n}_1}} = -0.0733$
$C_{n_{1_{n_2}}} = -0.0014$	$C_{n_{2n_2}} = -0.0051$
$C_{n_{1\dot{n}_2}} = 0.0765$	$C_{n_{2\dot{n}_2}} = -0.2588$
$C_{n_{1\delta_e}} = -0.19635$	$C_{n_{2\delta_e}} = 0.3939$

Note: (1) All coefficients are non-dimensional

(2) Data obtained from reference 3

$m = 7085$ slugs	$U_0 = 949$ ft/sec
$s = 1946$ ft^2	$\rho = 0.002378$ slugs/ft^3
$c = 15.33$ ft	$\bar{q} = 1071.754$ lbs/ft^2
$I_y = 5.8916 \times 10^6$ slug-ft^2	

2.3 Flight Director Equation

The total pitch angle time history that the pilot feels and sees, either on the outside horizon or the attitude indicator display, is given by (reference 4 and 5).

$$\theta_i(x_p,t) = \theta(t) - \sum_{i=1}^{2} \phi_i'(x_p)\eta_i(t) \qquad (2.22)$$

Figure 2.2 shows the pitch angle response to command input due to rigid-body motion and that due to the two lowest frequency elastic mode responses. Where x_p indicates pilot fuselage station and $\phi_i'(x_p)$ the slope of the i th symmetric elastic mode at that station.

The relative contribution of the elastic terms to the total pitch response increases as the natural frequencies of the modes decrease. Now the values of ϕ_1' and ϕ_2', which are obtained from B-1 data (reference 3), are as follows:

$$\phi_1' = 0.25$$

$$\phi_2' = 0.29$$

So equation (2.22) can be rewritten as

$$\theta_i(x_p,t) = \theta(t) - 0.25\eta_1 - 0.29\eta_2 \qquad (2.23)$$

2.4 Pitch Angle Error Equation

A pitch angle error results from the reference trajectory which is the commanded signal that the pilot is to follow. When the CRT is implemented, this pitch angle error would be a measured quantity. That is, the CRT would provide the aircraft with its present pitch angle and this would be compared with its desired pitch angle given by the reference trajectory. The difference

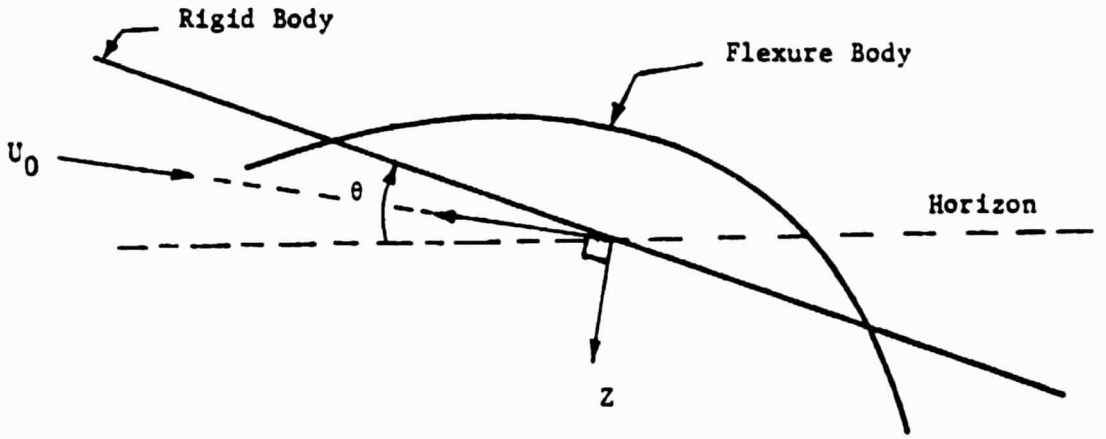

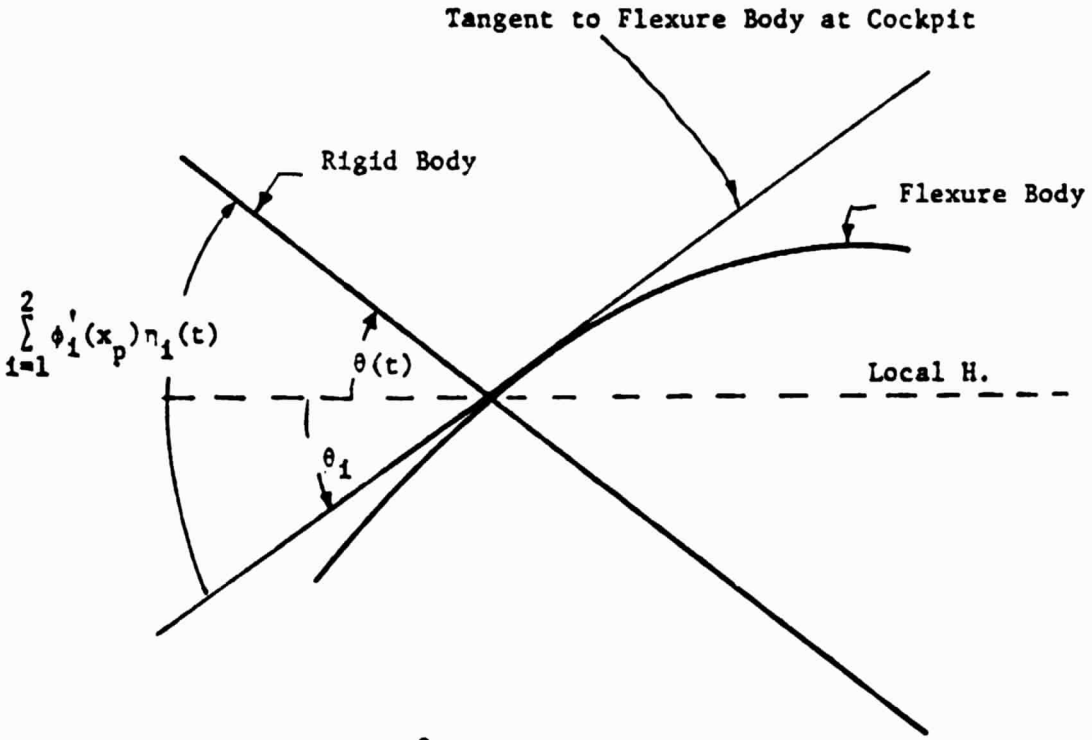

$$\theta_1 = \theta(t) - \sum_{i=1}^{2} \phi_i'(x_p)\eta_i(t)$$

Figure 2.2 Rigid and Elastic Pitch Angles

between the actual flight direction and the reference trajectory is the pitch angle error (see Figure 2.3).

The equation is as follows:

$$e_\theta = \theta_i - \theta_c \tag{2.24}$$

The pilot's job is to maintain this pitch angle error as close to zero as possible. The electronic attitude director is the display presently on the simulator built by William Seitz when the simulator was located in the M.E. school at Purdue (reference 13). A drawing of the display is shown in Figure 2.3. The dashed medium length line is attached to the face of a cathode ray tube (CRT) and represents the wings of the aircraft. The single long line moves up and down due to aircraft motion and represents the horizon. When the aircraft is pitched up, the horizon line is below the fixed aircraft symbol. The two short lines on the EADI are often referred to as a flight director. They move up and down to give pitch commands. The pilot's job is to keep the aircraft symbol centered in the two short lines. This display can be configured in two ways. The first is called a control director. With the control director, movement of the horizon line is directly related to movement of the control surface (control stick). When the pilot pulls the stick back (up elevator) the horizon line goes down. The displacement of the horizon line is related to control movements by a constant. As a result the two short lines

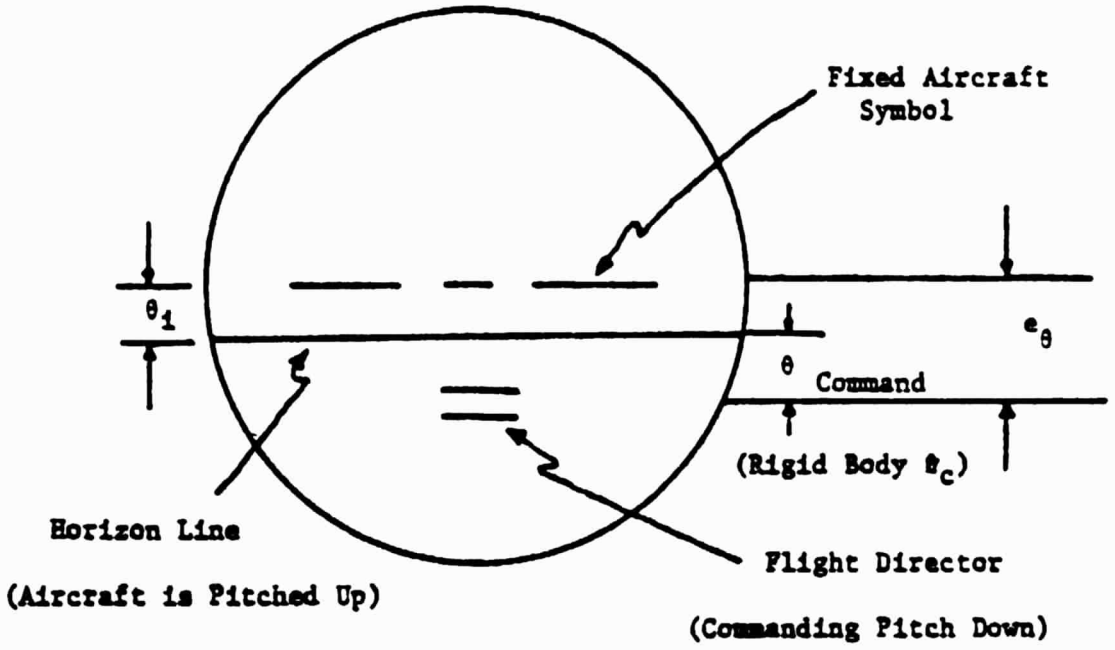

Figure 2.3a Electronic Attitude-Director Indicator (EADI)

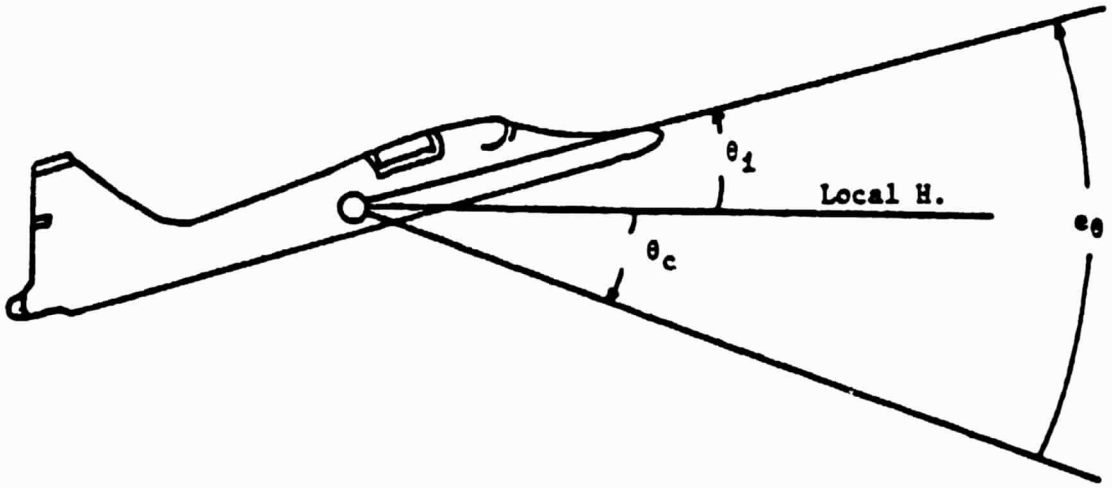

Figure 2.3b The Airplane Attitude Corresponding to Above EADI

command elevator deflection. The other configuration is a flight director. The horizon line and the two short lines are present in this mode also, they are just driven differently than the control director. A change in pitch angle (θ_i) produces a vertical displacement of the horizon line. As a result, movement of the two short lines commands change in pitch angle. The electronics driving the display are presently configured as a flight director, rather that control director, we have used it as a flight director in this work.

2.5 Summary Equations

Equations 2.21 can be written in matrix form in Table 2.3

Equations 2.21 are the longitudinal dynamics of the B-1 bomber at mach 0.85, sea level flight condition without the structural mode control system operating.

Equation 2.23 is the flight director equation and equation 2.24 is the pitch angle error equation.

These equations are all linear and are simulated on an analog computer in the piloted simulation used in this study.

Table 2.3 Equations of Motion in Matrix Form

$$\dot{x} = Ax + Bu$$

Where: $x = (u, \alpha, \theta, \dot{\theta}, \eta_1, \dot{\eta}_1, \eta_2, \dot{\eta}_2)^T$

$u = (\delta_e, \delta_t)^T$

$$A = \begin{bmatrix} -.025 & -25 & -32.2 & 0 & 0 & 0 & 0 & 0 \\ -.00065 & -1.205 & 0 & .943 & -.00905 & -.00021 & .00465 & .00015 \\ 0 & 0 & 0 & 1 & 0 & 0 & 0 & 0 \\ -.00228 & -7.0694 & 0 & -2.0195 & -.1845 & -.00744 & .2078 & .00697 \\ 0 & 0 & 0 & 0 & 0 & 1 & 0 & 0 \\ -.00147 & -737.92 & 0 & -133.268 & -177.447 & -1.1385 & -15.414 & .91534 \\ 0 & 0 & 0 & 0 & 0 & 0 & 0 & 1 \\ -.00399 & 757.29 & 0 & 55.951 & 6.985 & -.1219 & -465.523 & -.8491 \end{bmatrix}$$

$$B = \begin{bmatrix} 0 & .000141 \\ -.288 & 0 \\ 0 & 0 \\ -15.0541 & 0 \\ 0 & 0 \\ -2229.054 & 0 \\ 0 & 0 \\ 613.183 & 0 \end{bmatrix}$$

CHAPTER 3

DYNAMIC CHARACTERISTICS OF EIGHT CASES

3.1 General Description

In this study, the equation of motion as shown in equation (2.21) includes two elastic modes. The natural frequencies of the two elastic modes will be parametrically reduced. They are represented by eight cases which were each flown by several pilots. Dynamic characteristics for each of these eight cases will be specified by four modes: short period mode, phugoid mode, elastic mode 1, and elastic mode 2. The dynamics of these eight cases will be described in the following sections.

3.2 Dynamic Characteristics of Case 1, Case 2, and Case 3

In this section, only the natural frequency of elastic mode 1 (ω_1) was reduced and the natural frequency of elastic mode 2 (ω_2) was unchanged.

The value of ω_1 was varied from 13.59 rad/sec to 4.24 rad/sec. Three cases were chosen in this range of ω_1. The root-locus plot is shown in Figure 3.1.

The value of ω_1 is 13.59 rad/sec; it is the original value of ω_1. It was chosen as Case 1.

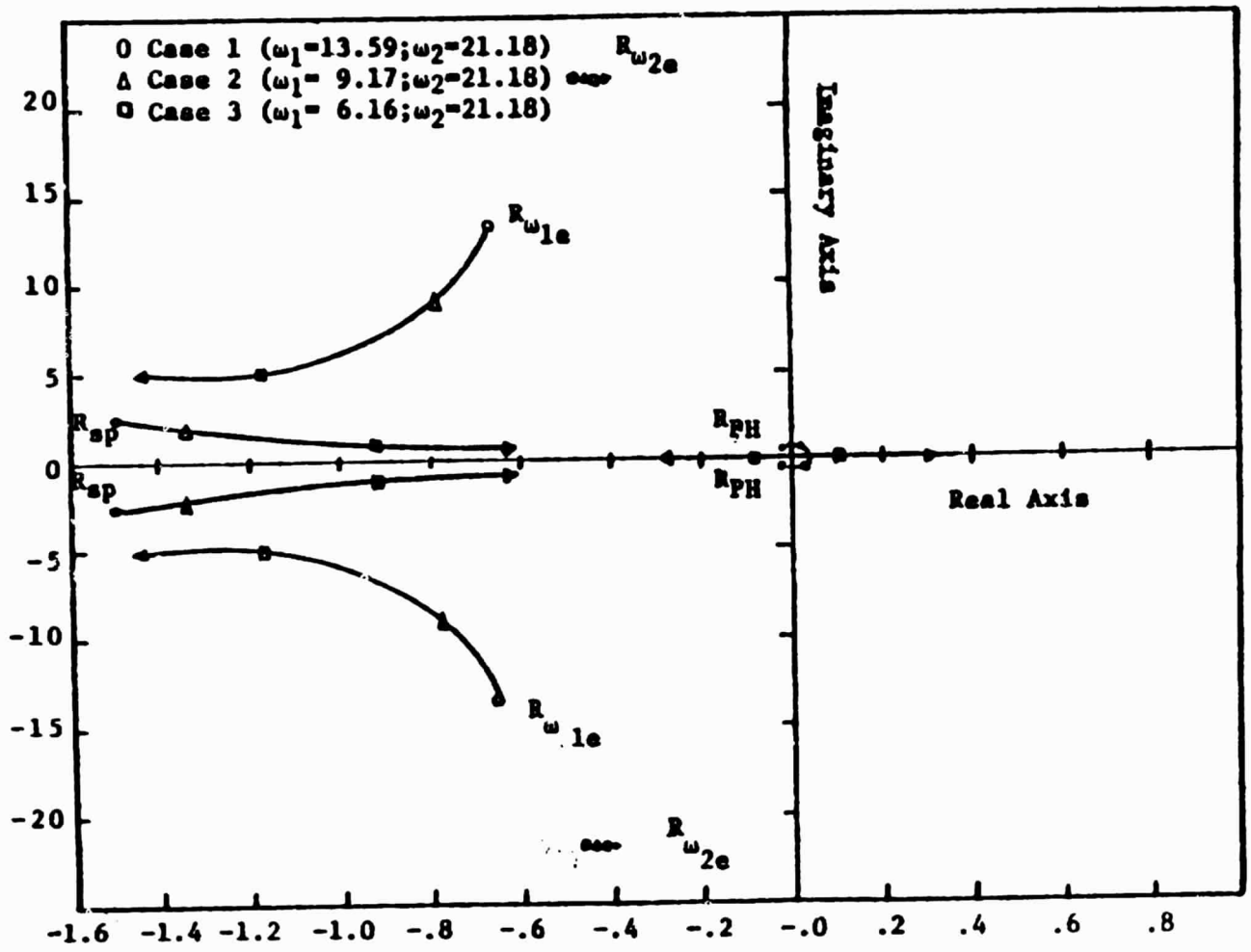

Figure 3.1 The Locus of Roots of Matrix A, Case 1, Case 2, Case 3, as a Function of Natural Frequency of Elastic Mode 1, ω_1

As the value of ω_1 was varied from 13.59 rad/sec to 9.21 rad/sec, all modes (phugoid, short period, elastic mode 1, elastic mode 2) were stable.

When the value of ω_1 is less than 9.21 rad/sec, the phugoid mode became unstable.

A value of ω_1 at 9.17 rad/sec was chosen as Case 2. A value of ω_1 at 6.16 rad/sec was chosen as Case 3, and the phugoid mode is unstable and non-oscillatory. This value of ω_1 was the lowest value that could be chosen for the pilot to fly. When the value of ω_1 was less than 6.16 rad/sec, the pilot could not control the unstable phugoid mode due to the mode interaction with elastic mode 1.

The dynamic characteristics of Case 1, Case 2, and Case 3 are shown in Tables 3.1, 3.2, and 3.3, respectively.

3.3 Dynamic Characteristics of Case 4

In this section, only the natural frequency of elastic mode 2 (ω_2, was reduced and the natural frequency of elastic mode 1 (ω_1) was unchanged.

The value of ω_2 was varied from 10.14 rad/sec to 2.83 rad/sec, and just one case was chosen in this range of ω_2. The root-locus plot is shown in Figure 3.2.

The value of ω_2 at 4.79 rad/sec was chosen as Case 4. This value of ω_2 was as low as could be chosen as previously discussed. If the value of ω_2 is larger than

Table 3.1 Dynamic Characteristics of Case 1

Case 1 (original case):

ω_1 = 13.59 rad/sec; $2\zeta_1\omega_1$ = 0.272

ω_2 = 21.18 rad/sec; $2\zeta_2\omega_2$ = 0.424

Parameter	Short Period	Phugoid	Elastic Mode 1	Elastic Mode 2
Roots	-1.498 ±2.373j	- 0.00139 ± 0.00708j	- 0.6583 ±13.295j	- 0.4603 ±21.349j
Coupled ur amped natural freq. (rad/sec)	2.806	0.07081	13.312	21.354
Coupled damping ratio	0.5339	0.01973	0.0494	0.0215
Coupled damped freq. (rad/sec)	2.373	0.0708	13.296	21.349
Time to half or twice Amp. (sec)	0.46	494.7	1.04	1.49
Period (sec)	2.648	88.7	0.47	0.29

Table 3.2 Dynamic Characteristics of Case 2

Case 2:

ω_1 = 9.17 rad/sec: $2\zeta_1\omega_1$ = 0.183

ω_2 = 21.18 rad/sec; $2\zeta_2\omega_2$ = 0.424

Parameter	Short Period	Phugoid	Elastic Mode 1	Elastic Mode 2
Roots	$-1.3468 \pm 2.1917j$	$+3.4536\times10^{-5} \pm 5.7305\times10^{-2}j$	$-7.7072\times10^{-1} \pm 8.7552j$	$-4.5676\times10^{-1} \pm 21.3511j$
Coupled undamped natural freq. (rad/sec)	2.5724	0.057305	8.7891	21.356
Coupled damping ratio	0.5235	-0.00060267	0.08769	0.0213
Coupled damped freq. (rad/sec)	2.19	0.057304	8.7552	21.3512
Time to half or twice Amp. (sec)	0.5124	19979.149	0.8953	1.5169
Period (sec)	2.8667	109.6447	0.7176	0.2943

Table 3.3 Dynamic Characteristics of Case 3

Case 3:

$\omega_1 = 6.16$ rad/sec; $2\zeta_1\omega_1 = 0.123$

$\omega_2 = 21.18$ rad/sec; $2\zeta_2\omega_2 = 0.424$

Parameter	Short Period	Phugoid	Elastic Mode 1	Elastic Mode 2
Roots	-9.2283×10^{-1} $\pm1.5093j$	$+9.0978\times10^{-2}$ -7.6723×10^{-2}	-1.1728 $\pm5.7485j$	-4.5568×10^{-1} $\pm21.352j$
Coupled undamped natural freq. (rad/sec)	1.7691		5.8669	21.357
Coupled damping ratio	0.5217		0.1999	0.021337
Coupled damped freq. (rad/sec)	1.5093		5.7485	21.3521
Time to half or twice Amp. (sec)	0.7476		0.5883	1.5142
Period (sec)	4.1631		1.0930	0.2943

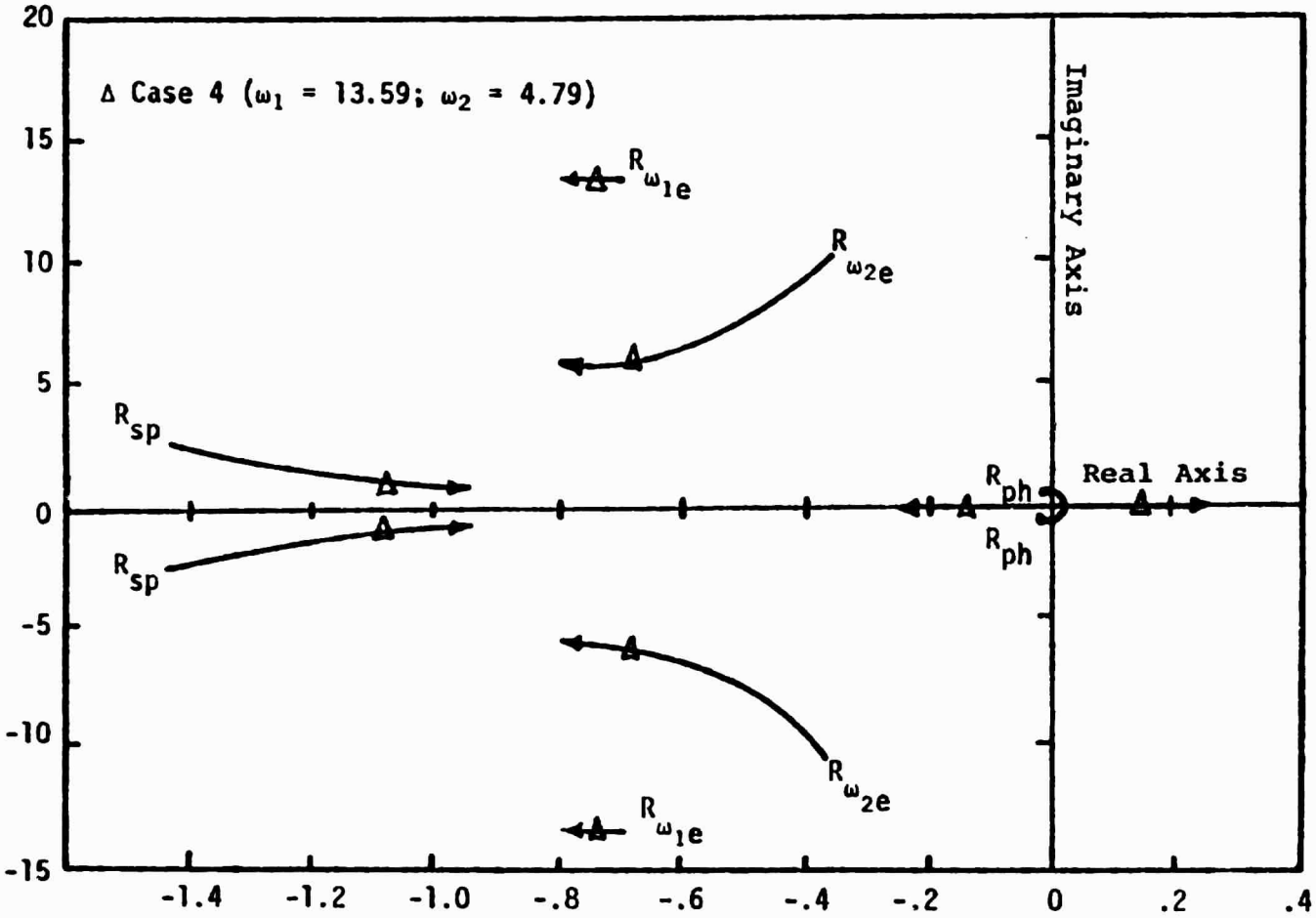

Figure 3.2 The Locus of Roots of Matrix A, Case 4, as a Function of Natural Frequency of Elastic Mode 2, ω_2

4.79 rad/sec, the situations would be the same as Case 1 and Case 2.

The dynamic characteristics of Case 4 are shown in Table 3.4.

3.4 Dynamic Characteristics of Case 5 and Case 6

Both natural frequencies of elastic mode 1 (ω_1) and elastic mode 2 (ω_2) were reduced.

The values of ω_1 and ω_2 were varied from 13.26 rad/sec to 4.89 rad/sec. Case 5 and Case 6 were chosen in this range for ω_1 and ω_2. The root-locus plot is shown in Figure 3.3.

When the values of ω_1 and ω_2 were 11.66 rad/sec, the phugoid mode was unstable and oscillatory. This was chosen as Case 5.

When the values of ω_1 and ω_2 were 6.93 rad/sec, the phugoid mode was unstable and non-oscillatory. This was chosen as Case 6. These values of ω_1 and ω_2 are as low as could be chosen in Case 6, as previously discussed.

The dynamic characteristics of Case 5 and Case 6 are shown in Tables 3.5 and 3.6, respectively.

3.5 Dynamic Characteristics of Case 7 and Case 8

The natural frequency of elastic mode 2 (ω_2) was varied from 10 rad/sec to 6.32 rad/sec while the natural frequency of elastic mode 1 (ω_1) was varied from 10 rad/sec to 12.61 rad/sec. The root-locus plot is shown in Figure 3.4.

Table 3.4 Dynamic Characteristics of Case 4

Case 4:

ω_1 = 13.59 rad/sec; $2\zeta_1\omega_1$ = 0.272

ω_2 = 4.79 rad/sec; $2\zeta_2\omega_2$ = 0.096

Parameter	Short Period	Phugoid	Elastic Mode 1	Elastic Mode 2
Roots	$-1.0819 \pm 1.1438j$	$+1.4654\times10^{-1}$ -1.3167×10^{-1}	$-7.0119\times10^{-1} \pm 13.251j$	$-6.7877\times10^{-1} \pm 5.9315j$
Coupled undamped natural freq. (rad/sec)	1.5745		13.270	5.9702
Coupled damping ratio	0.6872		0.05284	0.1137
Coupled damped freq. (rad/sec)	1.1438		13.251	5.7544
Time to half or twice Amp. (sec)	0.6377		9.8405	1.0165
Period (sec)	5.4931		4.7415	1.0919

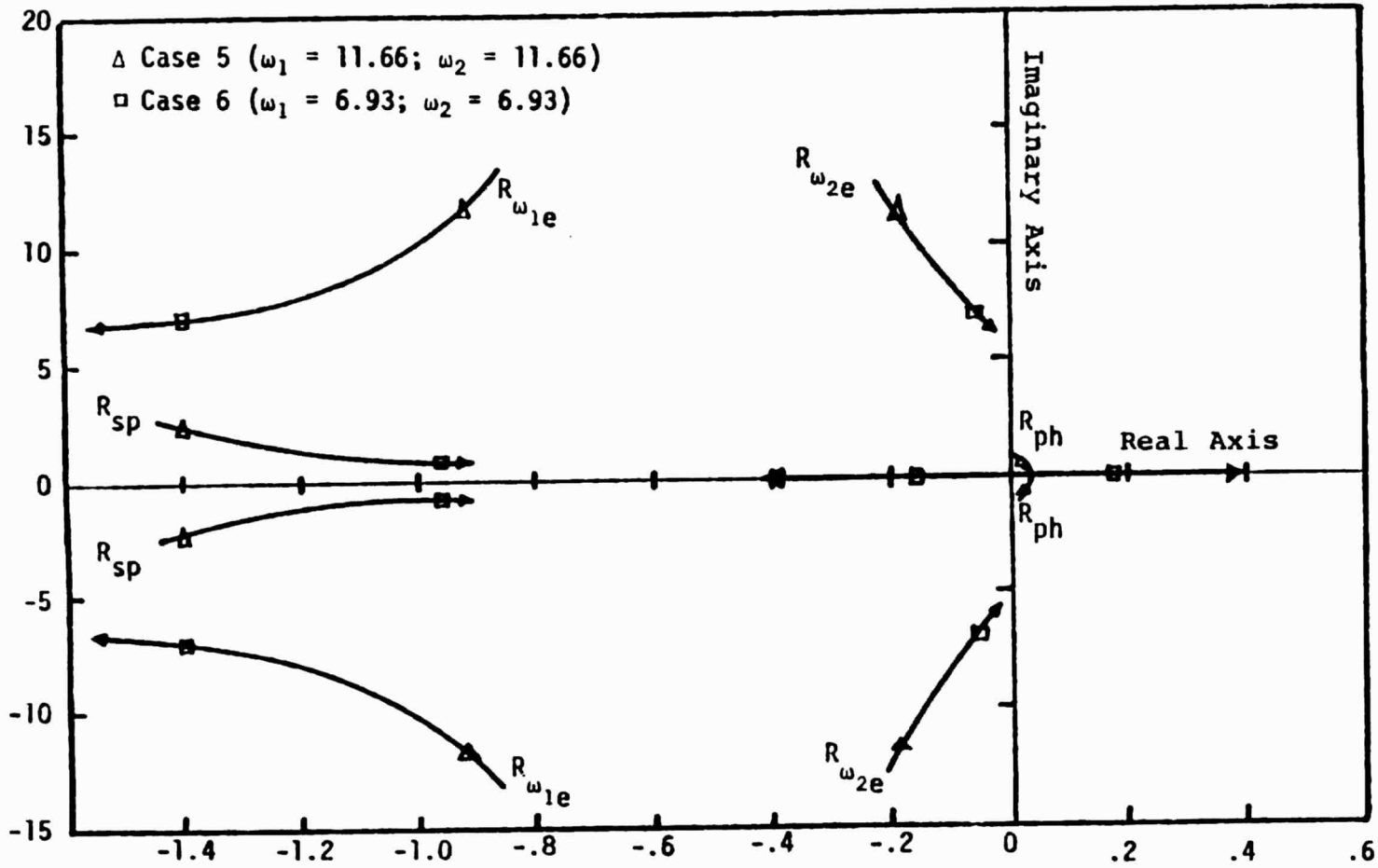

Figure 3.3 The Locus of Roots of Matrix A, Case 5, Case 6, as a Function of Natural Frequencies of Elastic Mode 1, ω_1, and Elastic Mode 2, ω_2

Table 3.5 Dynamic Characteristics of Case 5

Case 5:

ω_1 = 11.66 rad/sec; $2\zeta_1\omega_1$ = 0.233

ω_2 = 11.66 rad/sec; $2\zeta_2\omega_2$ = 0.233

Parameter	Short Period	Phugoid	Elastic Mode 1	Elastic Mode 2
Roots	$-1.4035 \pm 2.1671j$	$+6.0288\times10^{-6} \pm 5.3748\times10^{-2}j$	$-9.1264\times10^{-1} \pm 11.765j$	$-1.8770\times10^{-1} \pm 11.573j$
Coupled undamped natural freq. (rad/sec)	2.5819	0.053745	11.801	11.574
Coupled damping ratio	0.54359	-0.00011217	0.077338	0.01621
Coupled damped freq. (rad/sec)	2.1671	0.053745	11.7657	11.5725
Time to half or twice Amp. (sec)	0.4916	114454.8772	0.7560	3.6778
Period (sec)	2.8993	116.9073	0.5340	0.5429

Table 3.6 Dynamic Characteristics of Case 6

Case 6:

$\omega_1 = 6.93$ rad/sec; $2\zeta_1\omega_1 = 0.139$

$\omega_2 = 6.93$ rad/sec; $2\zeta_2\omega_2 = 0.139$

Parameter	Short Period	Phugoid	Elastic Mode 1	Elastic Mode 2
Roots	-9.0635×10^{-1} $\pm 9.7212\times10^{-1}j$	$+1.7581\times10^{-1}$ -1.5307×10^{-1}	-1.4072 $\pm 7.1942j$	-5.2984×10^{-2} $\pm 6.9716j$
Coupled undamped natural freq. (rad/sec)	1.3665		7.3305	6.9178
Coupled damping ratio	0.70279		0.19196	0.0075997
Coupled damped freq. (rad/sec)	0.9721		7.1942	6.9176
Time to half or twice Amp. (sec)	0.7185		0.4903	13.1246
Period (sec)	6.4634		0.8734	0.9083

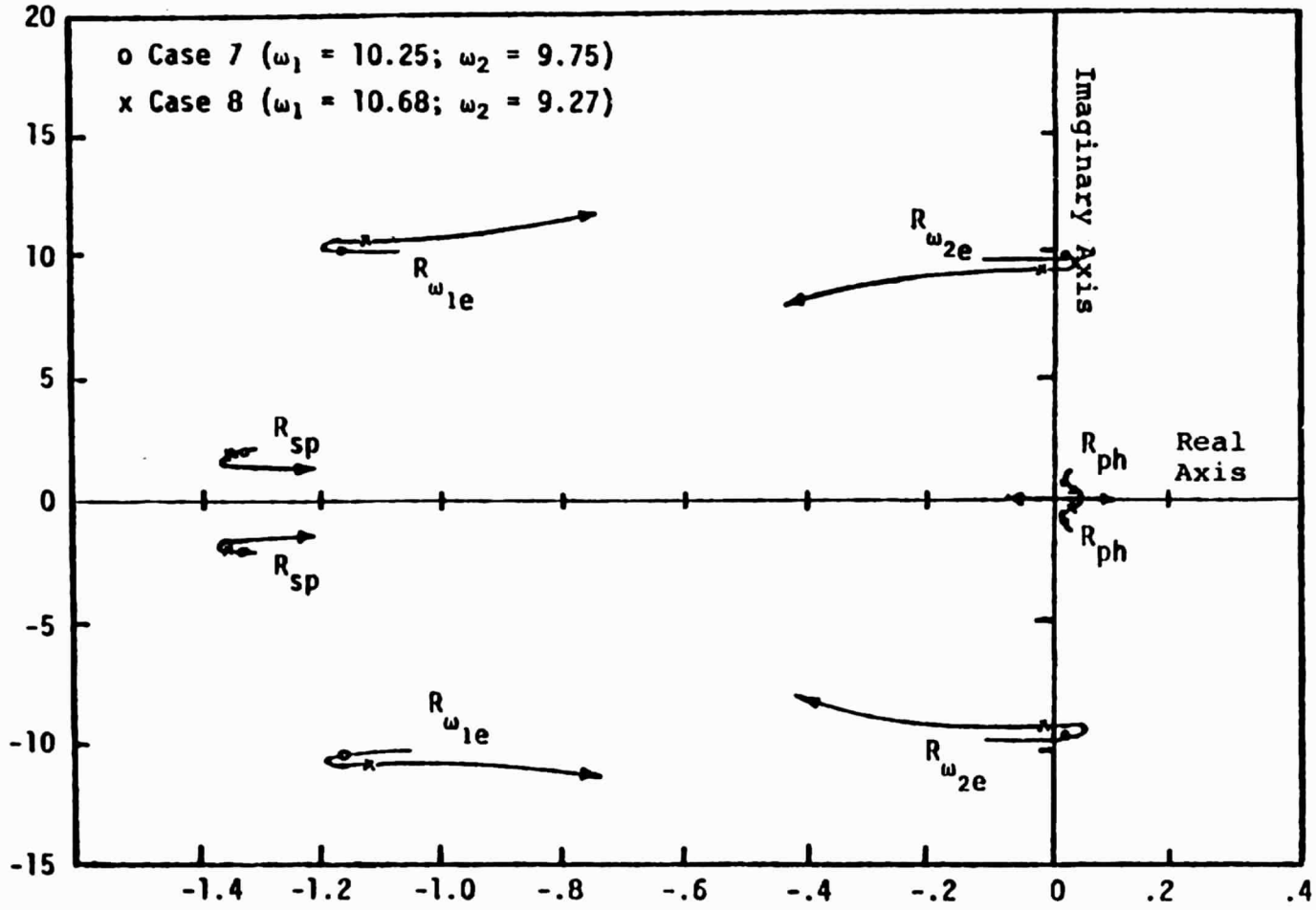

Figure 3.4 The Locus of Roots of Matrix A, Case 7, Case 8, as a Function of Natural Frequencies of Elastic Mode 1, ω_1, and Elastic Mode 2, ω_2

When the values of ω_1 and ω_2 were 10.25 rad/sec and 9.75 rad/sec, the phugoid mode and elastic mode 2 were unstable and oscillatory. This was chosen as Case 7.

When values of ω_1 and ω_2 were 10.68 rad/sec and 9.27 rad/sec, only the phugoid mode was unstable. This was chosen as Case 8.

The reason that both Case 7 and Case 8 were chosen was that their dynamic characteristics were quite similar, yet elastic mode 2 in Case 7 was a little unstable and that in Case 8 was stable. What would the handling qualities and pilot ratings in these two cases be?

The dynamic characteristics of Case 7 and Case 8 are shown in Tables 3.7 and 3.8, respectively.

3.6 Summary of Eight Cases

All these eight cases included most of the situations in which the handling qualities and pilot rating would be affected differently by the two elastic modes included in the model.

Each of the eight cases programmed in the analog computer driving the simulator displays was investigated to answer the questions posed.

Case 1, Case 2, and Case 3 were chosen when only the natural frequency of elastic mode 1 was reduced.

Case 4 was chosen when only the natural frequency of elastic mode 2 was reduced.

Table 3.7 Dynamic Characteristics of Case 7

Case 7:

ω_1 = 10.25 rad/sec; $2\zeta_1\omega_1$ = 0.205

ω_2 = 9.75 rad/sec; $2\zeta_2\omega_2$ = 0.195

Parameter	Short Period	Phugoid	Elastic Mode 1	Elastic Mode 2
Roots	$-1.3207 \pm 1.9964j$	$+1.3608\times10^{-3} \pm 2.8139\times10^{-2}j$	$-1.1554 \pm 10.168j$	$+4.2338\times10^{-3} \pm 9.8978j$
Coupled undamped natural freq. (rad/sec)	2.3937	0.028172	10.234	9.8978
Coupled damping ratio	0.55174	-0.048305	0.1129	-0.00042775
Coupled damped freq. (rad/sec)	1.9964	0.02814	10.1666	9.8345
Time to half or twice Amp. (sec)	0.5225	507.0366	0.5972	162.9748
Period (sec)	3.1473	223.2901	0.6179	0.6388

Table 3.8 Dynamic Characteristics of Case 8

Case 8:

$\omega_1 = 10.68$ rad/sec; $2\zeta_1\omega_1 = 0.214$

$\omega_2 = 9.27$ rad/sec; $2\zeta_2\omega_2 = 0.185$

Parameter	Short Period	Phugoid	Elastic Mode 1	Elastic Mode 2
Roots	$-1.3259 \pm 1.9876j$	$+1.3833\times10^{-3} \pm 2.5533\times10^{-2}j$	$-1.1404 \pm 10.284j$	$-5.1889\times10^{-3} \pm 9.7781j$
Coupled undamped natural freq. (rad/sec)	2.3893	0.02557	10.347	9.7781
Coupled damping ratio	0.55493	-0.054096	0.11021	0.00053066
Coupled damped freq. (rad/sec)	1.9877	0.02553	10.2839	9.7781
Time to half or twice Amp. (sec)	0.5204	498.8307	0.6051	132.9775
Period (sec)	3.1611	246.0852	0.6109	0.6426

Case 5 and Case 6 were chosen when both the natural frequencies of elastic mode 1 and elastic mode 2 were reduced.

Case 7 was chosen when elastic mode 2 was unstable.

Case 8 was chosen with its dynamic characteristics close to that of Case 7 but with elastic mode 2 stable.

Table 3.9 shows the coupled undamped natural frequencies and damping ratios of the rigid and elastic modes for each of the eight cases.

Table 3.9 Natural Frequencies and Damping Ratios of Eight Cases

Case #	ω_1 rad/sec	ω_2 rad/sec	ζ_{sp}	ω_{sp} rad/sec	ζ_{ph}	ω_{ph} rad/sec	ζ_{1e}	ω_{1e} rad/sec	ζ_{2e}	ω_{2e} rad/sec
1	13.59	21.18	0.5339	2.806	0.0197	0.0708	0.0494	13.312	0.0215	21.354
2	9.17	21.18	0.5235	2.5724	-0.00060267	0.0573	0.08769	8.7891	0.0213	21.356
3	6.16	21.18	0.5217	1.7691	Real Roots +0.090978 -0.076723		0.1999	5.8669	0.0213	21.357
4	13.59	4.79	0.6872	1.5745	Real Roots +0.14654 -0.13167		0.05284	13.270	0.1137	5.9702
5	11.66	11.66	0.5436	2.5819	-0.0001122	0.0537	0.0773	11.801	0.0162	11.574
6	6.93	6.93	0.7028	1.3665	Real Roots +0.17581 -0.15307		0.1919	7.3305	0.007599	6.9178
7	10.25	9.75	0.5517	2.3937	-0.0483	0.0282	0.1129	10.234	-0.0004277	9.8978
8	10.68	9.27	0.5549	2.3893	-0.0541	0.0256	0.11021	10.347	0.0005306	9.7781

CHAPTER 4

EXPERIMENT

4.1 Overview

A pilot in the loop simulation was performed to answer the following questions. Of the eight cases examined, which one results in the worse pilot performance? What are the pilot comments on each case? How well can pilots perform in these cases compared to the original case (Case 1)?

The eight cases previously discussed were used to answer these specific questions. They are:

(1) Does Case 1 provide good handling qualities and pilot rating?

(2) Are the handling qualities and pilot rating for Case 2 and Case 3 acceptable, in which only the natural frequency of elastic mode 1 is changed? The natural frequency of elastic mode 1 is changed to a greater extent in Case 3 than that in Case 2.

(3) Are the handling qualities and pilot rating for Case 4 acceptable, in which only the natural frequency of elastic mode 2 is changed?

(4) Are the handling qualities and pilot rating for Case 5 and Case 6 acceptable, in which both the natural frequencies of the elastic modes are changed?

(5) Are the handling qualities and pilot rating for Case 7 and Case 8 acceptable? Elastic mode 2 is slightly unstable in Case 7, but it is stable in Case 8.

4.2 Apparatus

A fixed base simulator was adapted to answer these questions. A block diagram of the apparatus involved in this test is shown in Figure 4.1. Two Applied Dynamics analog computers comprising 60 amplifiers were used to simulate the equations of motion, flight director equation, and command signal. The mathematical forms for these equations were presented in Chapter 2. A schematic diagram of this simulation is shown in Appendix.

The cockpit mockup contained a control stick, a throttle, vertical velocity indicator, airspeed indicator, angle-of-attack indicator, altimeter, and the electronic attitude-director indicator (EADI).

A control stick provides elevator input to the aircraft simulation. Springs produce a restoring force on the control stick to return it to a neutral position.

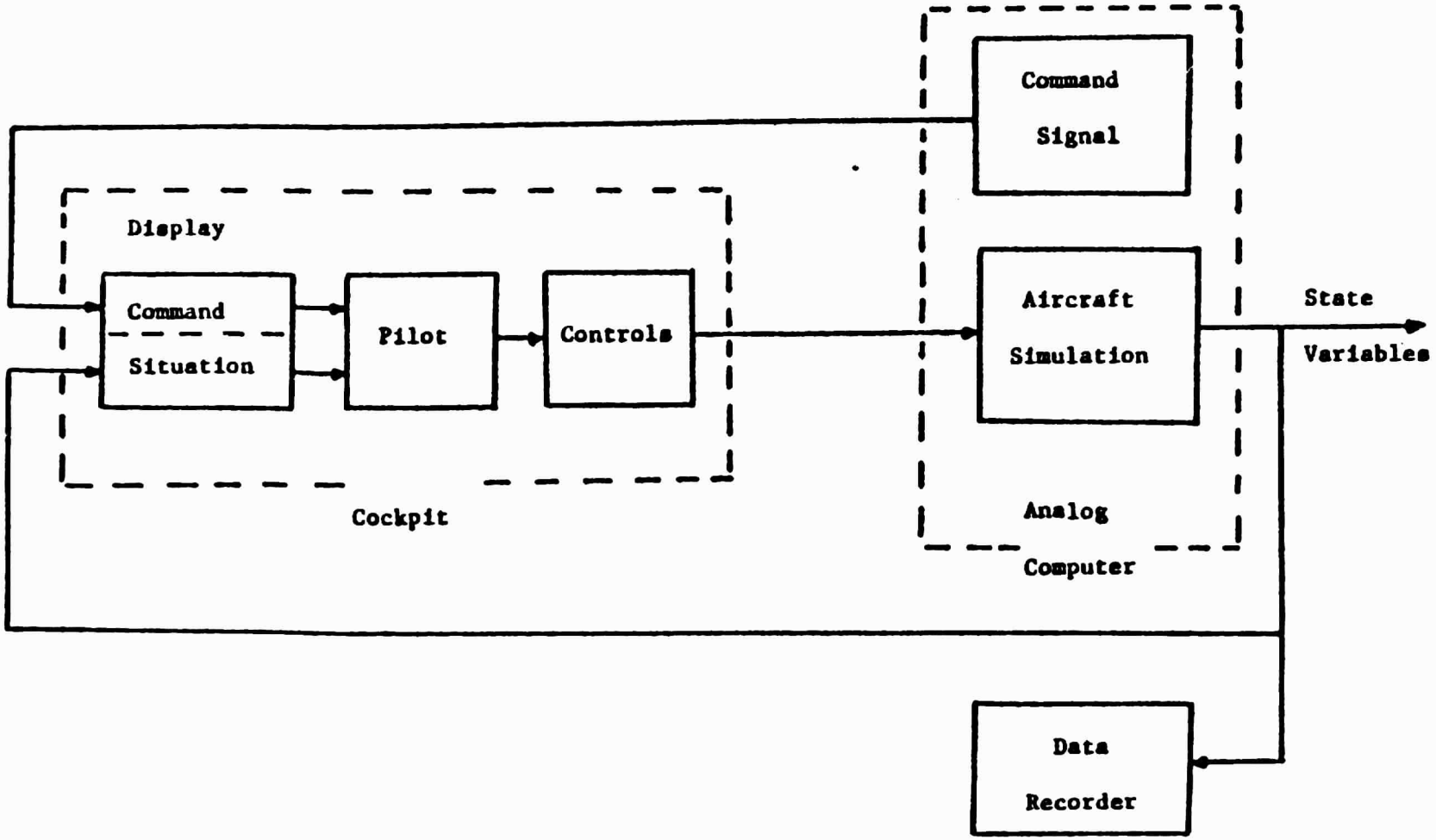

Figure 4.1 Block Diagram of Apparatus

The spring stiffness was suitable for pilots to fly (40 pounds for full elevator deflection). The resulting gradient provides good centering of the stick but does not require excessive force. The stick neutral position can be adjusted by using the elevator trim crank on the cockpit floor.

A throttle provides thrust input. Both of these inputs, elevator and throttle, are measured by the wiper of potentiometers mechanically connected to the movable controls. These measurements are then electrically connected to the input of operational amplifiers for use in the simulator.

Initially the aircraft is flying at 949 ft/sec at constant altitude with 0 degree flight path angle and $\alpha_0 = 3^\circ$, $\theta_0 = 0^\circ$, and up elevator $\delta_e = -6$ degrees.

The electronic attitude-direction indicator (EADI) vertical velocity, airspeed, altimeter, and angle-of-attack indicators are all visible. Description of the instruments is provided in reference 9.

The vertical velocity and angle-of-attack indicators are driven by miniature direct current (DC) servo systems that convert an analog computer DC voltage into an angular rotation of the needle within the instrument. The EADI is produced by drawing special symbols on cathode ray tubes (CRT). Details of the electronics are provided in reference 9.

4.3 Methodology

Data was recorded on four pilots flying each of eight cases during two separate approaches (replications). As a result, a total of 64 data runs were performed. This does not include all the time each pilot spent learning the simulator and practicing each case. This section describes the details of how the experiment was made including the cases arranged, instructions given, and data recorded.

To minimize the possibility of learning trends affecting the results of this experiment, the eight cases were presented in a different order to each pilot. The order they were presented in by means of random table (reference 12) is shown in Table 4.1.

Table 4.1 Order of Presentation of Cases

Pilot \ Run	1	2	3	4	5	6	7	8
P_1	C_2	C_6	C_5	C_8	C_4	C_1	C_3	C_7
P_2	C_1	C_2	C_6	C_7	C_8	C_5	C_3	C_4
P_3	C_4	C_7	C_8	C_2	C_3	C_6	C_5	C_1
P_4	C_1	C_3	C_6	C_2	C_4	C_8	C_7	C_5

Each of the four pilots was instrument rated. Their experience varied from private, military, to commercial. The average total flight hours was more

than 1800 hours. A detailed description of the simulator, each display, the task, and the purpose of the experiment was first distributed to each pilot. The task was described as "continuously maintain the tracking error of pitch angle e_θ as close to zero as possible while using throttle to maintain the trim airspeed value."

Each pilot spent from half an hour to one hour getting acquainted with the simulator. This involved learning the location and operation of each instrument and the dynamics and limitations of the aircraft. By this time each had a good understanding of the experiment and what was required.

After each pilot had been acquainted with the instruments, a two hour session of simulated flight for the first eight cases was conducted. Fifteen minutes were used for each case. Ten minutes of the fifteen minutes were spent in practicing with the particular case being examined. During this ten minutes the pilot flew at least twice - one for no command signal provided, another one for command signal provided. This command signal is shown in Figure 4.2. The deviation of pitch angle error was visible on the EADI; this acts as a means of determining the pilot's learning situation. When his performance had reached a plateau, the actual data run was taken. After these eight cases were finished, they were repeated in the same order. Thus, sixteen

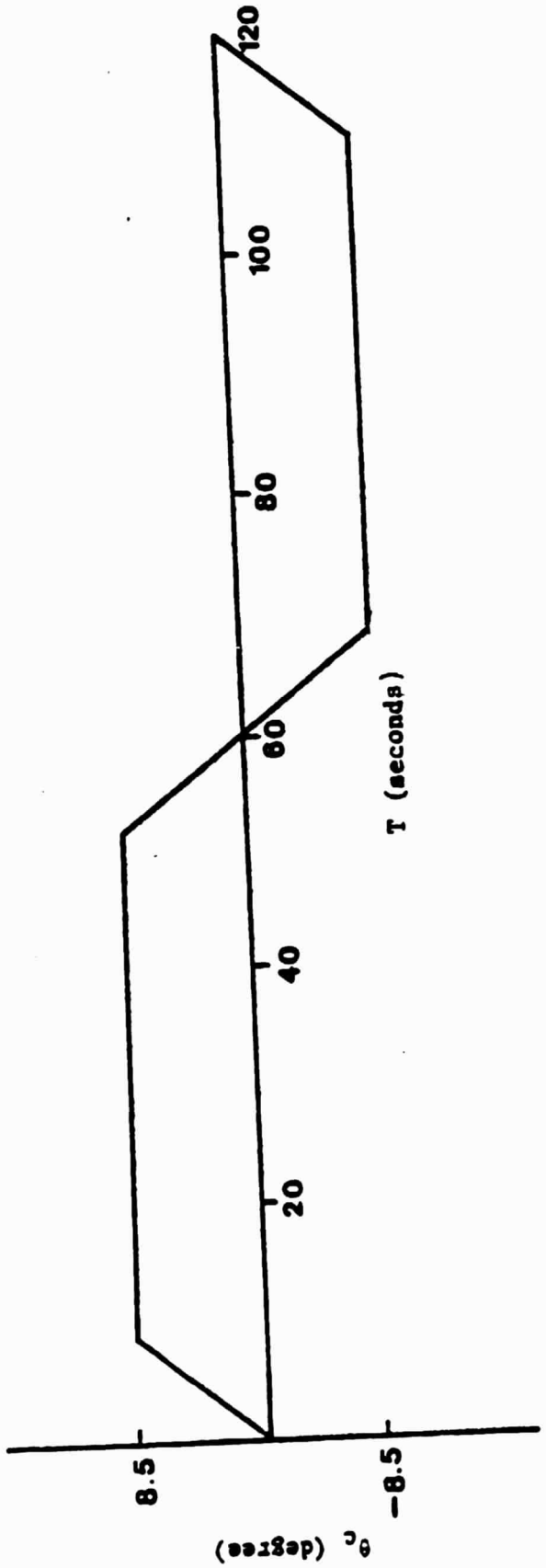

Figure 4.2 Command Signal

actual data runs were performed.

Each run begins with the aircraft at 562.2 knots at 6000 feet altitude. During the first 10 seconds, the pilot flies at a commanded 0.85 deg/sec pitch up. During the 10 second to 50 second period, the pilot makes any trim and power adjustments to keep the aircraft pitched up at 8.5 degrees. At 50 second, the pilot is given a command signal to start pitching down. After 20 seconds elapsed, the reference pitch angle is changed to -8.5 degrees. From the 70 second to 110 second period, the pilot makes any trim and power adjustments to keep the aircraft pitched down at -8.5 degrees. At 110 seconds, the pilot flies a commanded 0.85 deg/sec pitch up. At 120 seconds the experiment is completed.

In computing work, the tracking error, which was recorded by FM recorder, was sampled ten times per second and converted to digital words. The root mean square (RMS) of the tracking error was then computed off-line. The analysis was done later off-line by using a mini-computer. Because each pilot by observing the EADI knew how much the aircraft symbol was off the command signal, he was always aware of how well he was doing. Also time histories of six pertinent parameters were recorded by three two-parameter strip chart recorders.

Each pilot was given a questionnaire at the completion of the experiment. It requested he list comments

on each case and assign a Cooper-Harper rating to each case. A tape recording was also made of verbal comments.

CHAPTER 5

RESULTS

5.1 Method of Analysis

This chapter compares the performance in each of the eight cases, including an analysis of the mean tracking performance, a Cooper-Harper rating, and comments by the pilots. Root mean square (RMS) error of some quantity is frequently used to evaluate tracking performance. In this study, RMS pitch angle error is used. The magnitude of the RMS pitch angle error is an indication of how well the pilots followed the trajectory The task as described to the pilots was to "maintain the pitch angle error as small as possible." As a result, average RMS error is the most appropriate measure of performance.

One must be careful when comparing the mean performance because of the experimental nature of obtaining the results and variability of the pilots. For example, suppose one obtained results where the mean performance of system A is one unit better than system B, but the standard deviation for each was 10 units. One could not say with much confidence that system A was better than system B. With such large variance in the results the mean of A could have accidentally been better than the

mean of B. The technique of Analysis of Variance is a method for determining the probability that the results were due to chance.

Sixty-four observations of the RMS pitch angle error, C_{ij}, are shown in Table 5.1. The notation C_{ij} is used to denote the RMS pitch angle error for each observation. Subscript i is the row number corresponding to pilot performance while subscript j is the column number corresponding to case number. Two sets of observations were made for each pilot, thus there are two rows corresponding to each pilot. $\bar{C}_j$ denotes the mean of RMS pitch angle error in jth case; $\bar{C}$ is the overall mean. Analysis of variance (reference 10 and 11) was performed on the tracking error of pitch angle and is shown in Table 5.2. Degree of freedom means freedom to vary. Degrees of freedom for total cases are the number of observations in total minus 1 or 63; degrees of freedom for "between" cases are the number of cases minus 1 or 7; degrees of freedom for "within" cases are the sum of the number of observations within each minus 1 or 56. Table 5.2 indicates that the differences in performance among the cases were statistically significant at the 0.01 level. F ratio is a non-dimensional quantity that reflects the probability that the indicated results are due to chance. The F ratio is interpreted by use of the F table (reference 11). This table is entered with the number of

Table 5.1 64 observations of RMS Pitch Angle Error

Pilot \ Case i,j	C_1 1	C_2 2	C_3 3	C_4 4	C_5 5	C_6 6	C_7 7	C_8 8
P_1 1	0.0177	0.0234	0.0711	0.0257	0.0205	0.1119	0.0220	0.0185
P_1 2	0.0285	0.0052	0.1082	0.0246	0.0509	0.1488	0.00851	0.0179
P_2 3	0.0053	0.0038	0.1061	0.0309	0.0274	0.0651	0.0141	0.0052
P_2 4	0.0113	0.0256	0.1077	0.0291	0.0226	0.0796	0.0369	0.0339
P_3 5	0.0408	0.0284	0.0824	0.0381	0.0382	0.1033	0.0220	0.0232
P_3 6	0.0186	0.0190	0.0784	0.0360	0.0214	0.1748	0.0575	0.0272
P_4 7	0.0192	0.0240	0.1121	0.0395	0.0180	0.1791	0.0261	0.0199
P_4 8	0.0191	0.0166	0.1258	0.0396	0.0114	0.1943	0.0190	0.0160

$\bar{C}_1$=0.0201 $\bar{C}_2$=0.0183 $\bar{C}_3$=0.0990 $\bar{C}_4$=0.0331 $\bar{C}_5$=0.0263 $\bar{C}_6$=0.1321 $\bar{C}_7$=0.0258 $\bar{C}_8$=0.0202

$\bar{C}$ = .0481

Table 5.2 Analysis of Variance

Source of Variation	Degree of Freedom	RMS Pitch Angle Error		
		Sum of square	Mean square	F-ratio
Between cases	7	0.10637	0.01518	35.201**
Within cases	56	0.02425	0.00043	
Total	63	0.13042		

where: **significant at .01 level

"Between" sum of square: $\sum_{i=1}^{8} \sum_{j=1}^{8} (\bar{C}_j - \bar{C})^2$

"Within" sum of square: $\sum_{i=1}^{8} \sum_{j=1}^{8} (C_{ij} - \bar{C}_j)^2$

"Total" sum of square: $\sum_{i=1}^{8} \sum_{j=1}^{8} (C_{ij} - \bar{C}_j)^2$

"mean squares" are obtained by dividing each of the sum of squares by its respective number of degrees of freedom

$$\text{"F-ratio"} = \frac{\text{mean square for "between" cases}}{\text{mean square for "within" cases}}$$

degrees of freedom for the greater mean square across the top and with the number of degrees of freedom in the lesser mean square on the left-hand side. For this problem, we go over to 7 and down to 56. In that location we observe that the value of F needed for significance at 1 percent point is 2.98. Since our obtained F is greater than this, this means that the chance that these means of cases are significantly different is 99 percent.

It should be emphasized that statistical significance and engineering significance are two different concepts. Statistical significance refers to the probability that the results are due to chance whereas engineering significance refers to the benefits due to increased performance. Statistical significance can be well quantified whereas engineering benefit is frequently very subjective.

Unfortunately, Analysis of Variance tells only if the differences among C_1, C_2, C_3, C_4, C_5, C_6, C_7, and C_8 are statistically significant. What is of interest is a comparison among the cases. This can be done by using the "Newman-Keuls Test" (reference 12). This test determines how large a difference is required between two means for this difference to be statistically significant. The difference reflects the magnitude of the means and variances and the number of pilots and replications performed. That is, as the means or variances increase,

so must the difference between the means to maintain the same level of significance.

5.2 Comparison of Cases

Table 5.3 gives the means and standard deviations for each of the different cases among all pilots. For example, the average RMS pitch angle error for the four pilots over two replications C_1 is .0201 radians. These results are plotted in Figure 5.1. The diamond represents the mean RMS pitch angle error and the dashed lines extend to the one sigma deviations.

Table 5.4 is the result of the "Newman-Keuls Test" discussed previously. It presents the required differences between means for various levels of significance. Comparing the difference seen in Table 5.3 with those required as presented in Table 5.4 indicates that Cases C_6 and C_3 were each significantly worse than C_4, C_5, C_7, C_8, C_1, C_2. In between C_6 and C_3, C_6 was significantly worse than C_3. While C_4 appears to be worse than C_5, C_7, C_8, C_1, C_2, the difference was not statistically significant. The above indicates that the pilots do equally well for cases C_4, C_5, C_7, C_8, C_1, and C_2 in controlling the pitch angle error. In eight cases, C_6 is the worst, C_3 is the second worst.

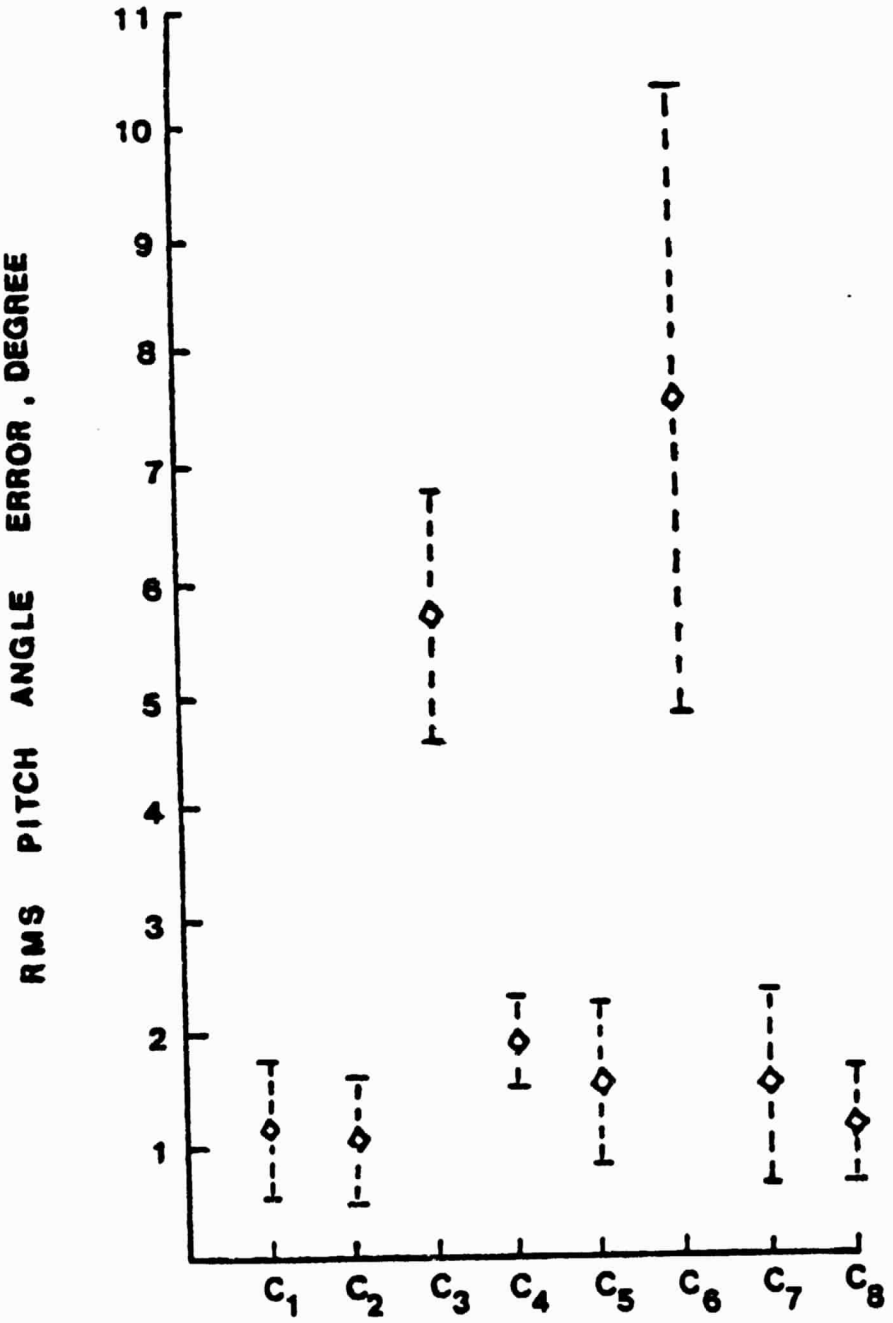

Figure 5.1 Tracking Performance Versus Cases

Table 5.3 Summary of Results

	RMS pitch Angle Error Radian (Degree)	
	Mean	Std. Dev
Case C_1	.0201 (1.1516)	.0107 (.6131)
Case C_2	.0183 (1.0485)	.0093 (.5329)
Case C_3	.0990 (5.6723)	.0192 (1.1001)
Case C_4	.0331 (1.8965)	.0060 (.3438)
Case C_5	.0263 (1.5069)	.0126 (.7219)
Case C_6	.1321 (7.5688)	.0488 (2.7960)
Case C_7	.0258 (1.4782)	.0153 (.8766)
Case C_8	.0202 (1.1574)	.0084 (.4813)

Table 5.4 Required Difference in Means for Statistical Significance

Level of Significance	RMS Pitch Angle Error
Cases	radian (degree)
0.01 level	0.0311 (1.78)

The pilots were asked to assign to each case a Cooper-Harper rating for the tracking task and the aircraft as simulated. The means and standard deviations of these ratings are shown in Figure 5.2. C_1, C_2, C_5, and C_8 were good; C_7 required minimal pilot compensation; C_4 required minimal to moderate pilot compensation; C_3 required considerable to maximum compensation; C_6 required extensive to unacceptable compensation. This result is consistent with the tracking performance just presented. That is, C_6 is worse than C_3 which is much worse than C_4, C_7, C_8, C_5, C_2, and C_1. Here, C_4 is worse than C_7 which is worse than C_8, C_5, C_2 and C_1. C_1, C_2, C_5, and C_8 show little difference.

Another important criterion for determining the "worst" case is the pilot's preferences and criticisms about the cases. In response to the request, "compare the difficulty of flying Case 1 with the difficulty of the other seven cases," the pilots' answers centered around:

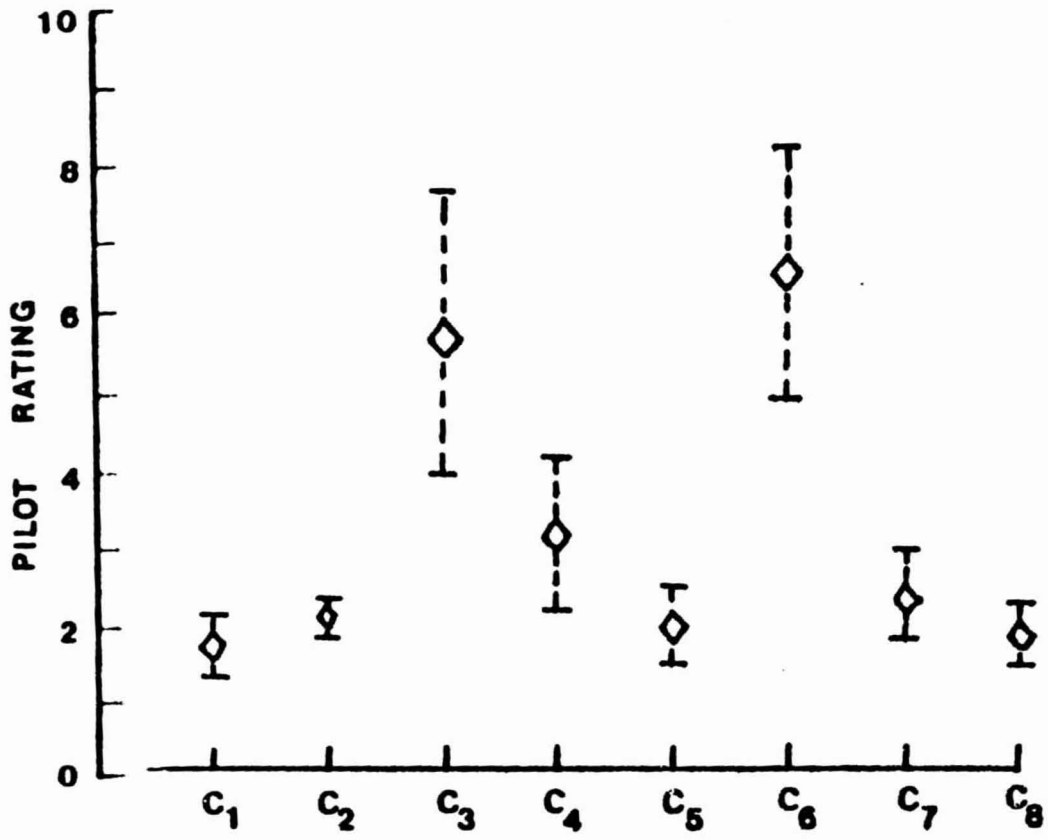

PILOT RATING	PILOT COMPENSATION REQUIRED
8	UNACCEPTABLE
7	MAXIMUM
6	EXTENSIVE
5	CONSIDERABLE
4	MODERATE
3	MINIMAL
2	UNNEEDED

Figure 5.2 Cocper-Harper Ratings

C_1 = easy

C_2 = about same as C_1

C_3 = difficult

C_4 = slightly difficult

C_5 = about same as C_1

C_6 = more difficult

C_7 = slightly difficult

C_8 = about same as C_1

In addition, the pilots gave the following comments on the eight cases:

C_1:

(1) Nothing objectionable on the pitch attitude tracking at all. Very nice case.

(2) It was very easy to hold it precisely. No control effort at all.

(3) I felt this was the easiest case to control.

(4) I find no problem with the dynamic characteristics of this simulator.

C_2:

(1) Fairly easy one to fly-it was not difficult to hold the command symbol right with the airplane symbol. There was very little oscillation in it; very little control motion is required to follow the command.

(2) Pitch-wise a little more difficult than C_1 situation, but still able to maintain pretty much within the limits.

(3) The slight continuous oscillation plus the slight lagging control response would be acceptable in a long flight in the event that it did not get worse.

C_3:

(1) It did appear to be unstable in rigid-body dynamics. It was fairly difficult to hold the airplane symbol in the command box. It took fairly strong amounts of concentration to keep the symbol in the command box and if you got away from it a little way, it was very difficult to get it back.

(2) Unable to maintain within the pitch limits and had a problem of pilot-induced oscillations due to large elastic amplitude oscillations.

(3) This case was very objectionable due to the extreme lag in the change of pitch of the aircraft following a control movement.

C_4:

(1) Not quite as easy as some of the others, but it was not difficult at all either. Did seem to be a little unstable in rigid-body dynamic motion. It took a little more forward pressure to do it and stick has a very stiff spring in the forward motion.

(2) The pitch control was a little bit annoying. There did not seem to be quick enough response with the cyclic stick.

C_5:

(1) That was about exactly the same difficulty as Case 2; that means its very easy to fly and was exactly the same in all characteristics as the Case 2.

(2) Handling characteristics seem to be pretty good there - not too much excursion on pitch.

(3) Has very good pitch control.

C_6:

(1) That was tremendous amount of oscillation in it. The control motions were very exaggerated and it took large displacement on the control to try to follow up.

(2) Difficulty maintaining within the limits pitch wise, probably out on pitch.

(3) The cyclic response is not real good. Abrupt immediate large changes produces disastrous effects.

(4) With the severity of these oscillations, caused in this case, it would be virtually uncontrollable.

C_7:

(1) It was not terribly difficult to track the command box. There was noticeable oscillation, due to the elasticity; but again, it was not too difficult to ignore that and to fly simply the rigid portion of the pitch profile.

(2) That was easier to control. The oscillation due to elasticity was of main annoyance.

(3) In this case, the aircraft would be quite controllable without an augmentation.

C_8:

(1) I believe that this case is the same as Case 2 and Case 5 - not difficult at all to fly the command profile. This one I can hold almost at the center all the time precisely. There was a little more

oscillation involved due to elasticity apparently, but it was high enough frequency that it was easier to ignore that and simply to fly the rigid-body of the profile that is coming from the command.

All three performance measures, tracking error, Cooper-Harper Rating, and pilots' comments agree that C_6 was generally worse than C_3 which was worse than C_4, C_7, C_8, C_5, C_2, and C_1.

Table 5.5 shows the summary for each of eight cases in three performance measures.

5.3 Time Histories

A sample time history of six pertinent variables (θ_i, e_θ, $\eta_1\phi_1'$, $\eta_2\phi_2'$, θ, δ_e) is examined for each of the eight cases to see the how and why of the differences in pitch angle error. All the sample time history plots did not come from one pilot.

Figure 5.3 is a sample time history plot for Case 1. During the 120 seconds flying time, θ_i is almost the same as θ, due to the fact that $\eta_1\phi_1'$ and $\eta_2\phi_2'$ are small and do not contribute much to θ_i. This case approaches that of a rigid-body. e_θ was easy to zero out; that is, the dynamic characteristics are good.

Table 5.5 Summary of Tracking Error, Cooper-Rating, and Pilots' Comments

No. of Case	Tracking Error		Pilot Rating	Pilots' Comments
	Radian	Degree		
C_1	.0201	1.1516	1.6	Good
C_2	.0183	1.0485	2.0	Very little oscillation
C_3	.0990	5.6723	5.9	Large amplitude oscillation, difficult control
C_4	.0331	1.8965	3.1	Not very easy to control
C_5	.0263	1.5069	2.0	A little more oscillation than C_2
C_6	.1321	7.5688	6.7	Tremendous amount of oscillation
C_7	.0258	1.4782	2.3	An annoying oscillation
C_8	.0202	1.1574	1.9	A little more oscillation than C_2

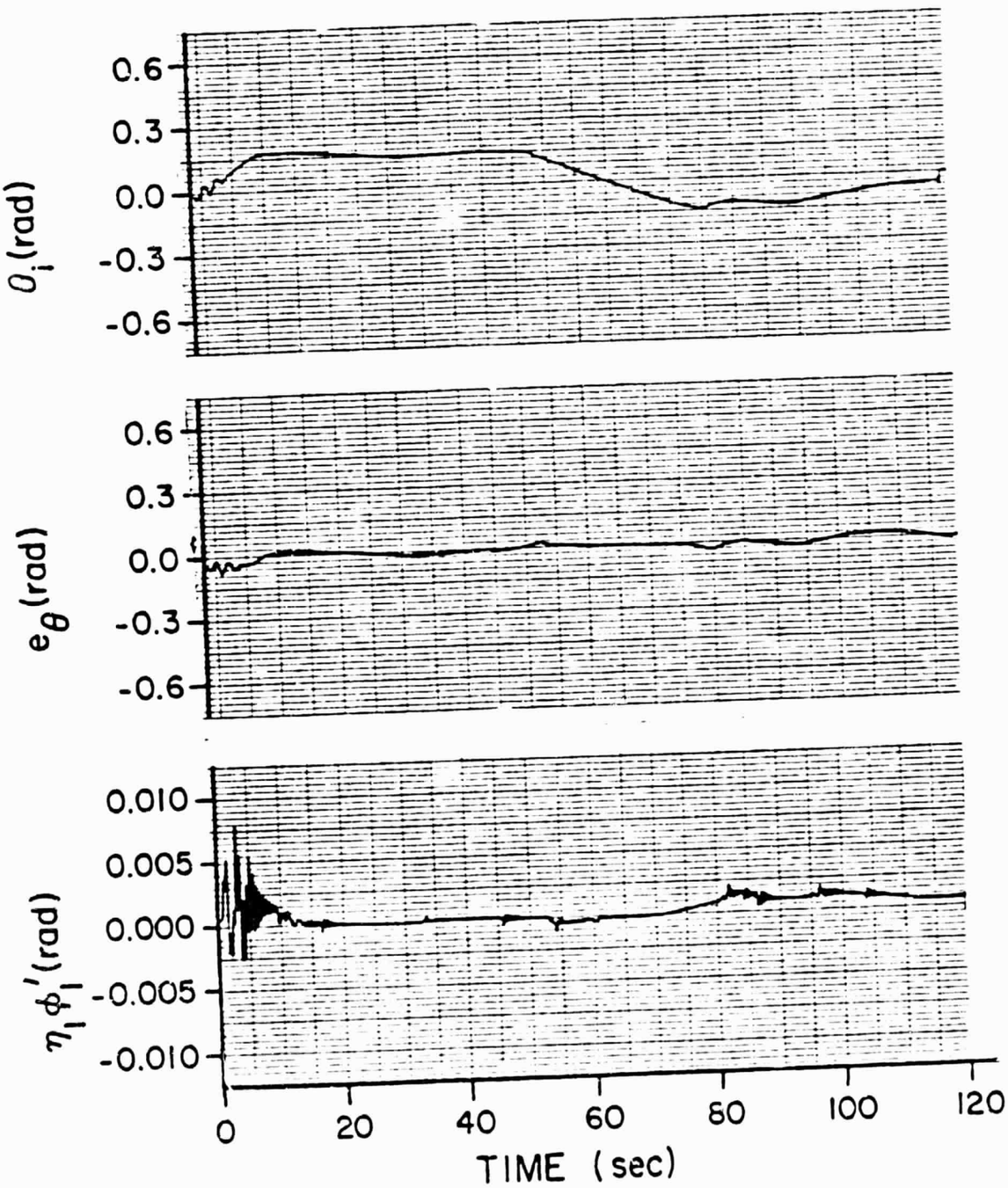

Figure 5.3A Sample Time History - Case 1

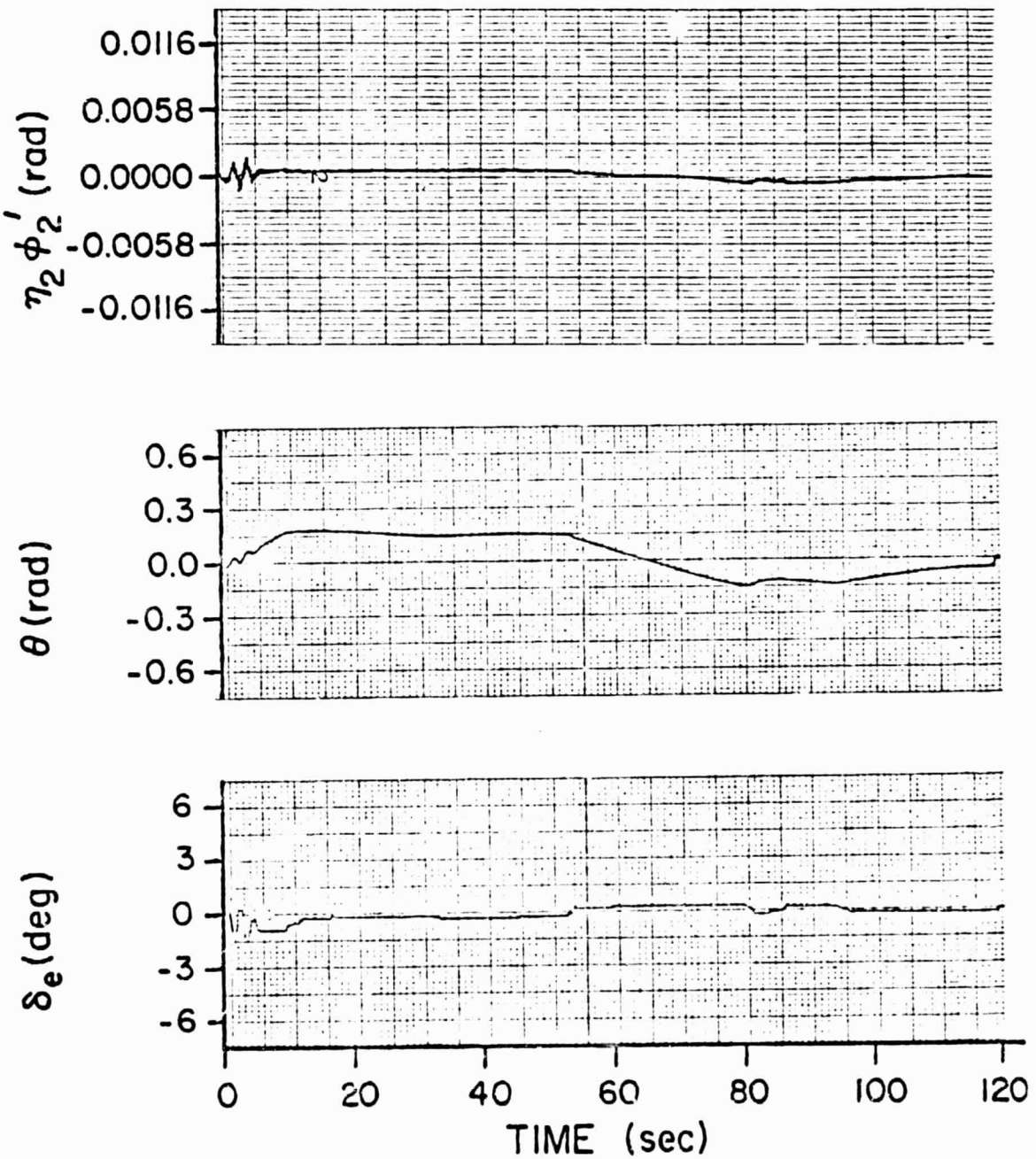

Figure 5.3B Sample Time History - Case 1

Future work should use a full state feedback control law to place the roots of the characteristic equation at precise values for each case. The rigid-body dynamics could then be maintained at their nominal values and the elastic mode coupled frequencies placed where desired. This would ensure that the pilot ratings would be based on the relative amplitudes of rigid and elastic pitch angle responses as presented on the EADI and not on poor rigid-body dynamics.

BIBLIOGRAPHY

1. Bisplinghoff, R. L., Ashley, H., and Halfman, R. L., Aeroelasticity, Addison-Wesley, 1955.

2. Chalk, C. R., et al, "Background Information and User Guide for MIL-F-8785B (ASG), 'Military Specification - Flying Qualities of Piloted Airplanes,'" AFFDL-TR-69-72, Air Force Flight Dynamics Laboratory, Wright-Patterson AFB, Ohio, 1969.

3. Wykes, J. H., "B-1 Flexible Vehicle Equations of Motion For Ride Quality, Terrain Following, and Handling Qualities Studies," Internal Document TFD-71-430-1, North American Rockwell, Los Angeles, CA, 1971, revised 1973.

4. Swaim, R. L., "A Proposal for Research on Handling and Ride Qualities of Large Flexible Control-Configured Aircraft," Purdue University, July 1, 1974.

5. Crother, C. A., Gabelman, B., and Langton, D., "Structural Mode Effects on Flying Qualities in Turbulence," AFFDL-TR-73-88, August 1973.

6. Swaim, R. L. and Fullman, D. G., "Prediction of Elastic-Airplane Longitudinal Dynamics from Rigid-Body Aerodynamics," Journal of Aircraft, Vol. 14, No. 9, September 1977, pp. 868-873.

7. Roskam, J., Flight Dynamics of Rigid and Elastic Airplanes, The University of Kansas, Lawrence, Kansas, 1973.

8. Swaim, R. L., "Aircraft Handling Qualities and Stability Augmentation Systems," unpublished notes.

9. Silverthorn, J. T., "An Aircraft Simulator for the Study of Pilot-Display Interactions," School of Aeronautics and Astronautics, Purdue University, March 1975.

10. Carlborg, F. W., Introduction to Statistics, Scott, Foresman and Company, 1968, pp. 208-223.

11. Dowine, N. M., Heath, R. W., Basic Statistical Methods, Harper and Row, 1965, pp. 215-222

12. Anderson, Virgil L., and McLean, Robert A., Design of Experiments, Marcel Dekker, Inc., New York, 1974.

13. Seitz, W. R., "Flight Director Design for an STOL Aircraft," Ph.D. thesis, Purdue University, August 1971.

14. Blakelock, J. H., Automatic Control of Aircraft and Missiles, John Wiley and Sons, 1965.

APPENDIX

APPENDIX

ANALOG SIMULATION

The equations presented in Table 2.3 and equation (2.23) and (2.24) were normalized by the scale factors given in Table A.1 and implemented on two Applied Dynamics analog computers. Patching diagrams of these equations are shown in Figures A.1 - A.8. Included are the longitudinal equations of motion, flight director equation, pitch command input, and control inputs. These differential equations were used to obtain the tracking error of pitch angle, angle-of-attack, airspeed, vertical speed, and altitude. Table A.2 gives the potentiometer settings used for this simulation, and Table 2.3 gives the potentiometer settings for each of the eight cases.

Figure 5.4 is a sample time history plot for Case 2. In this case $\eta_1\phi_1'$ is slightly greater than that in Case 1. However, its contribution to θ_i is still small. e_θ can still be zeroed out easily.

Figure 5.5 is a sample time history for Case 3. In this case $\eta_1\phi_1'$ is much greater than that in Case 2, causing greater contribution to θ_i. Significant changes in θ_i are observed. The pilot has difficulty zeroing out e_θ; e_θ is large. The difficulty in operating this case can be seen from the great movement of the control stick (as shown by δ_e plot). Dynamic characteristics are poor in this case.

Figure 5.6 is a sample time history plot for Case 4. In this case the major contribution to θ_i is $\eta_2\phi_2'$. However, the effect of $\eta_2\phi_2'$ is less than that of $\eta_1\phi_1'$ in Case 3; θ_i in this case is smaller than θ_i in Case 3. Even though the natural frequency of elastic mode 2 is reduced to a greater extent than that of elastic mode 1 in Case 3, the effect on θ_i is less. e_θ is slightly greater than that in Case 2. The pilot has to work harder to control the pitch angle (as shown by δ_e plot).

Figure 5.7 is a sample time history plot for Case 5. Both $\eta_1\phi_1'$ and $\eta_2\phi_2'$ contribute to θ_i. However, their magnitudes are small. The pilot still can zero it out; e_θ is not quite as large. e_θ has an oscillation of small magnitude due to the interaction between $\eta_1\phi_1'$ and $\eta_2\phi_2'$.

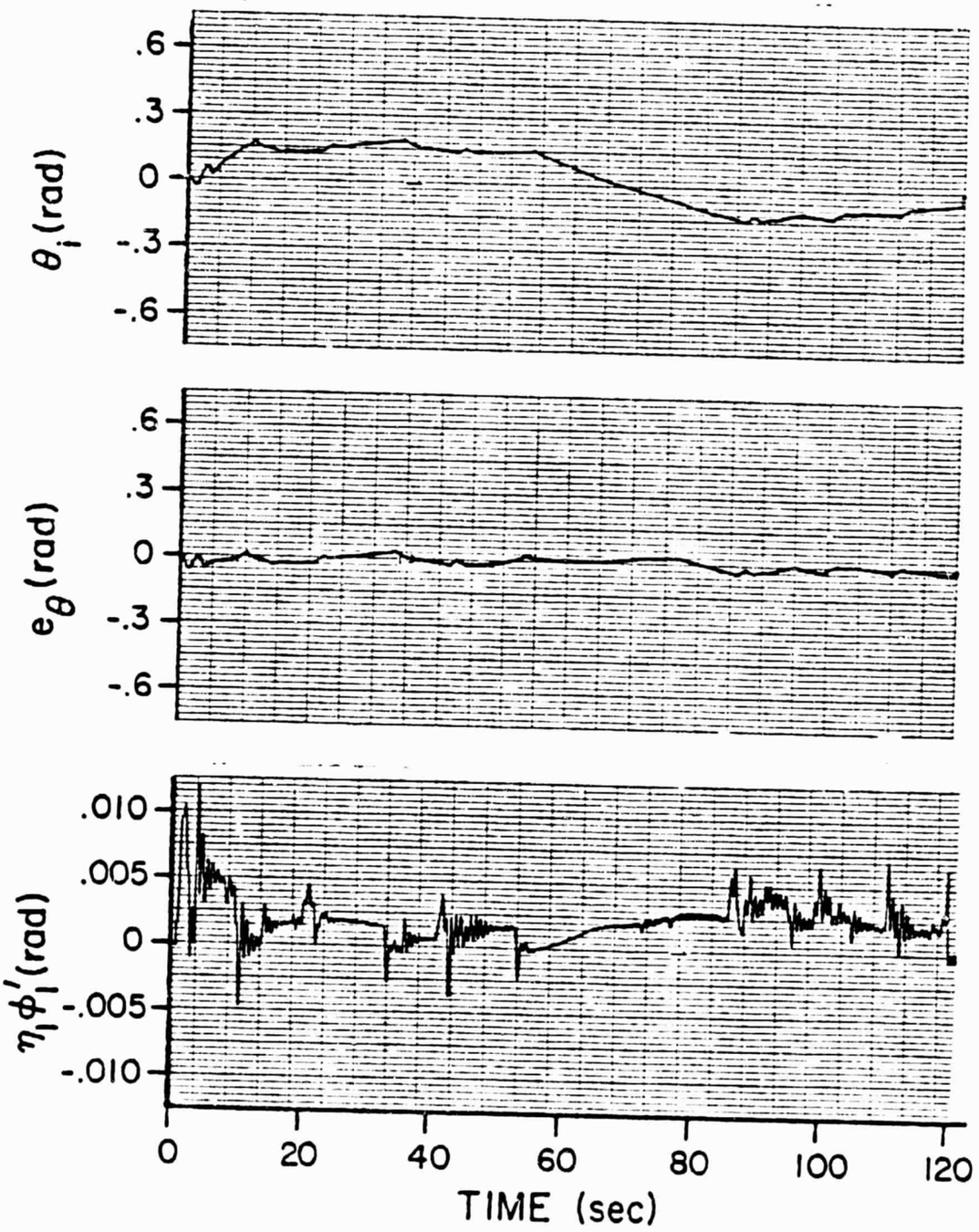

Figure 5.4A Sample Time History - Case 2

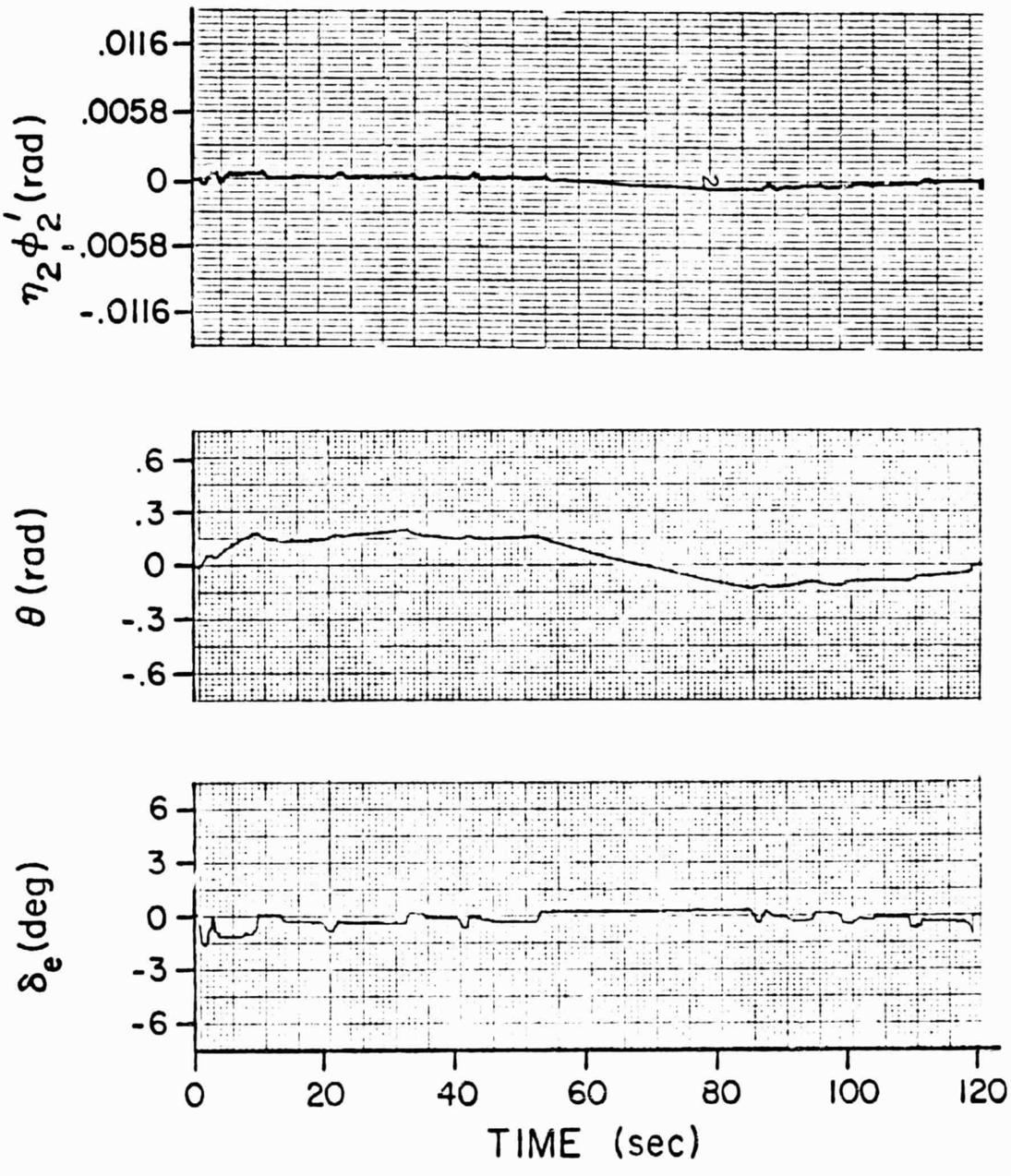

Figure 5.4B Sample Time History - Case 2

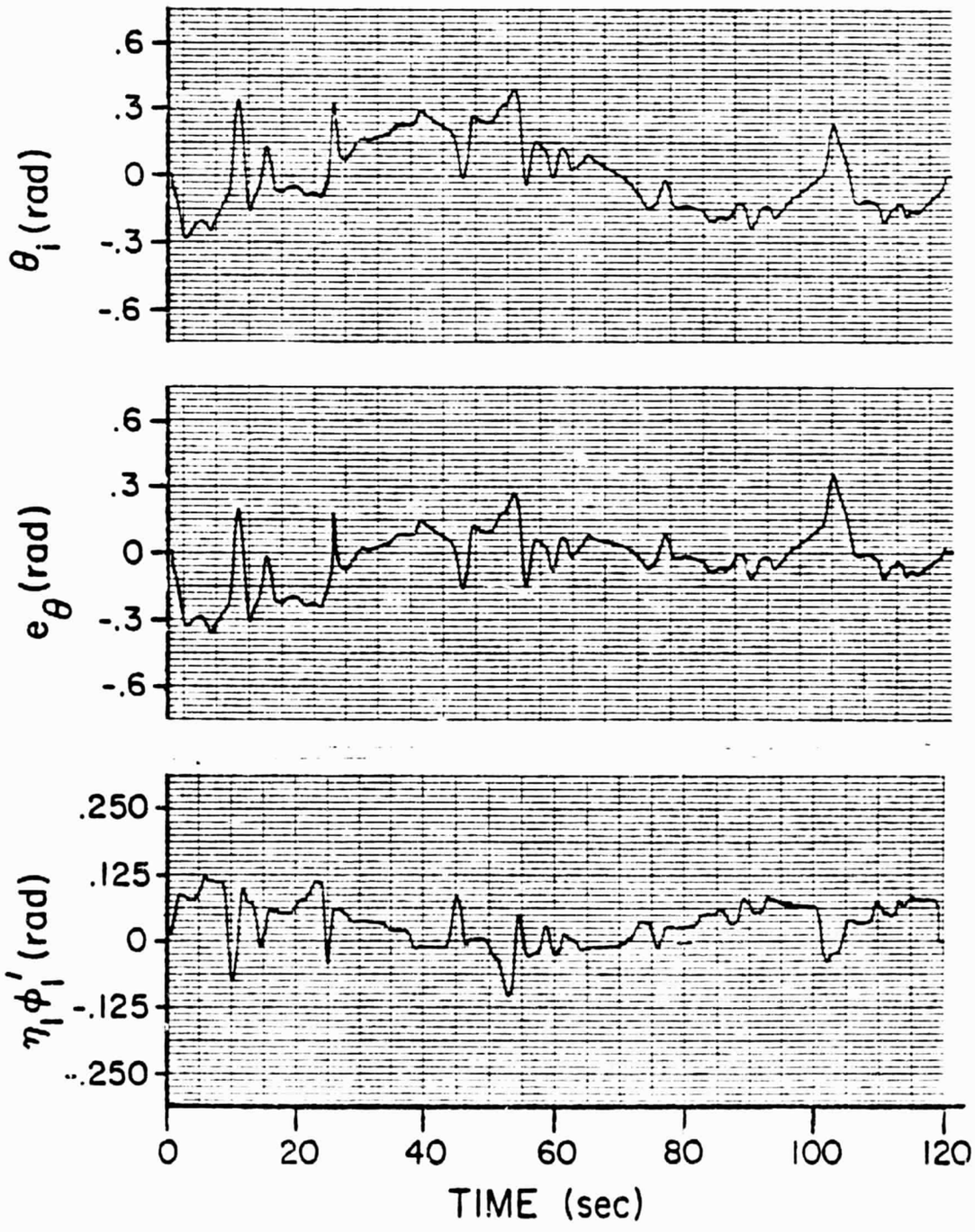

Figure 5.5A Sample Time History - Case 3

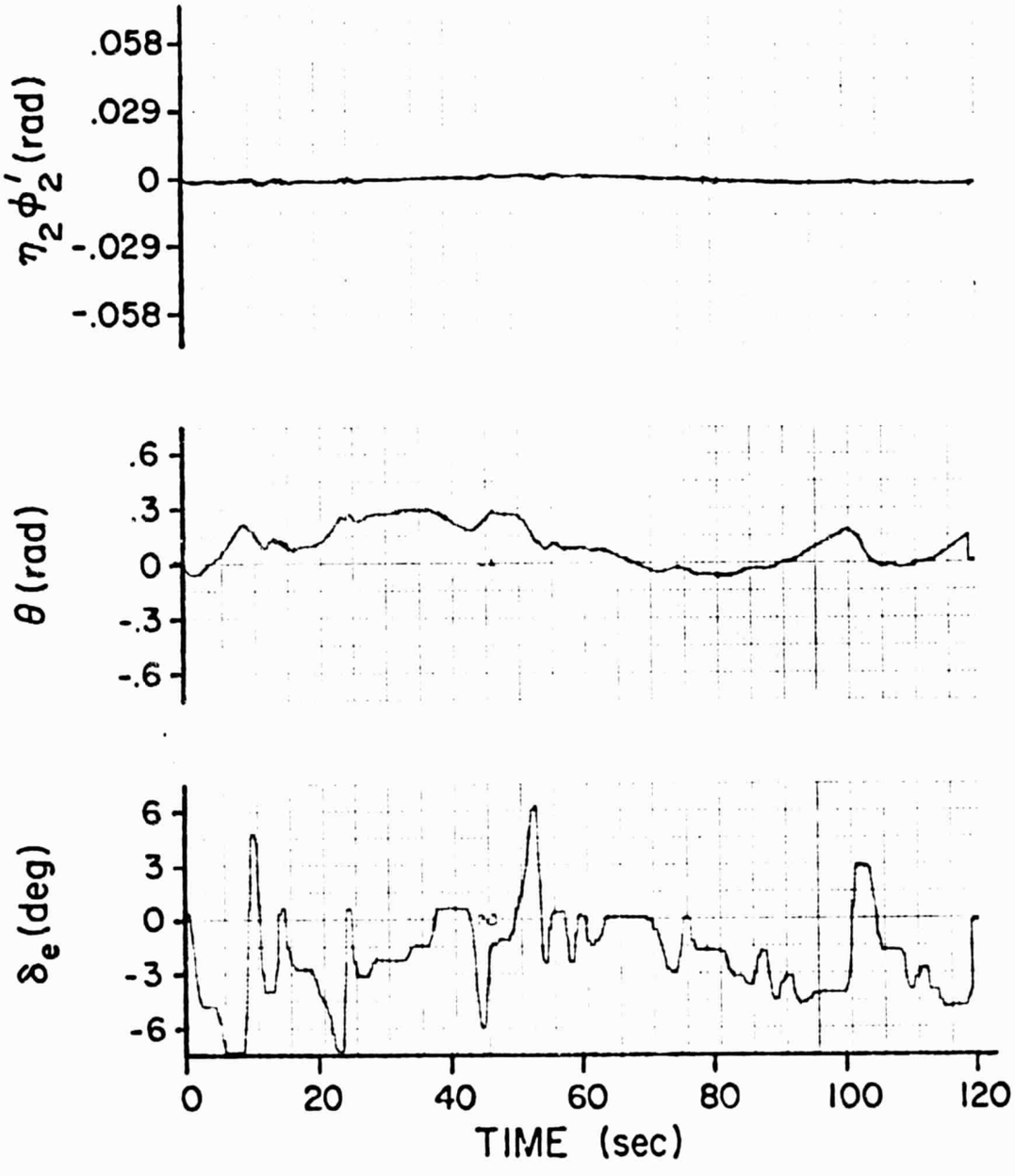

Figure 5.5B Sample Time History - Case 3

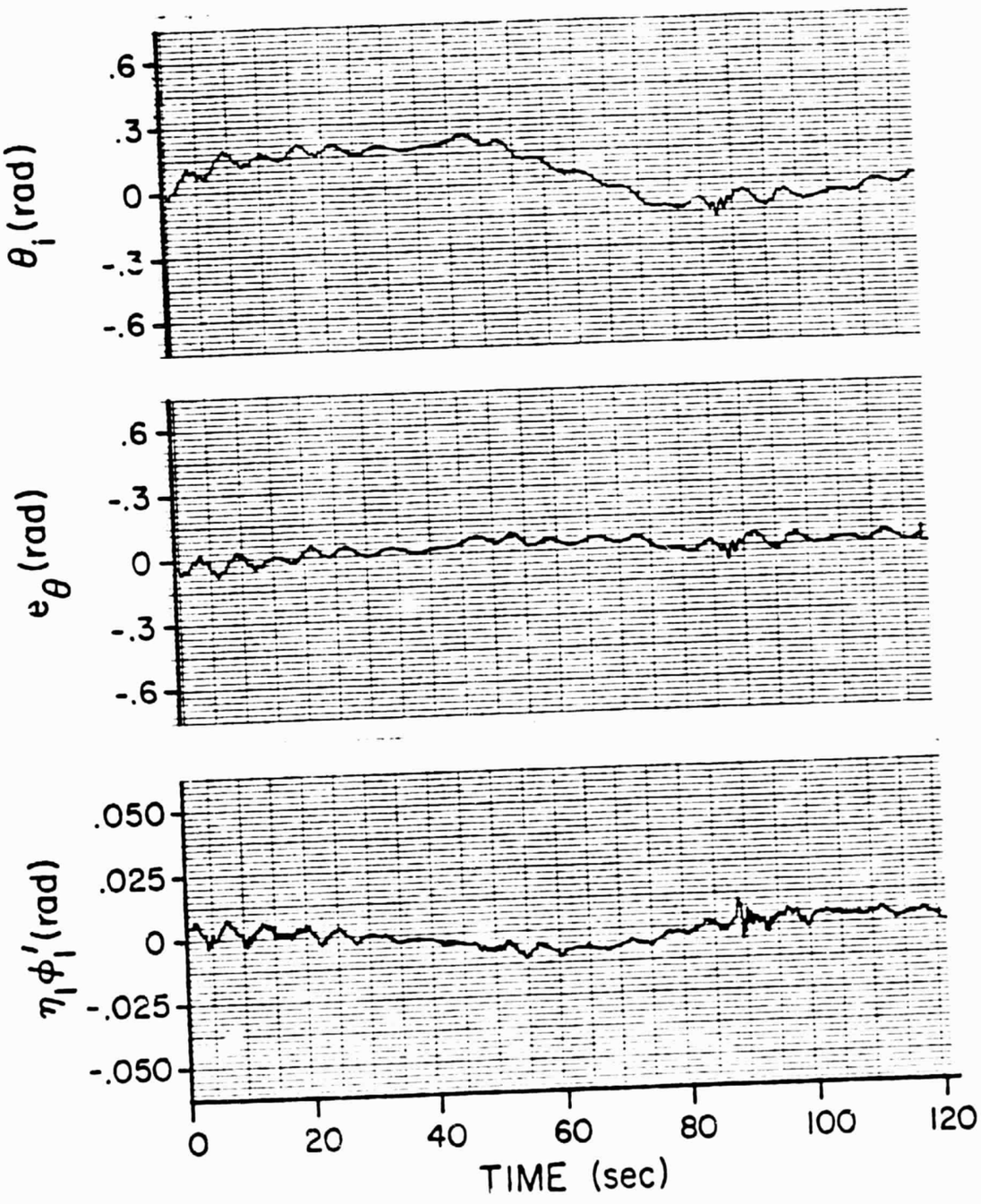

Figure 5.6A Sample Time History - Case 4

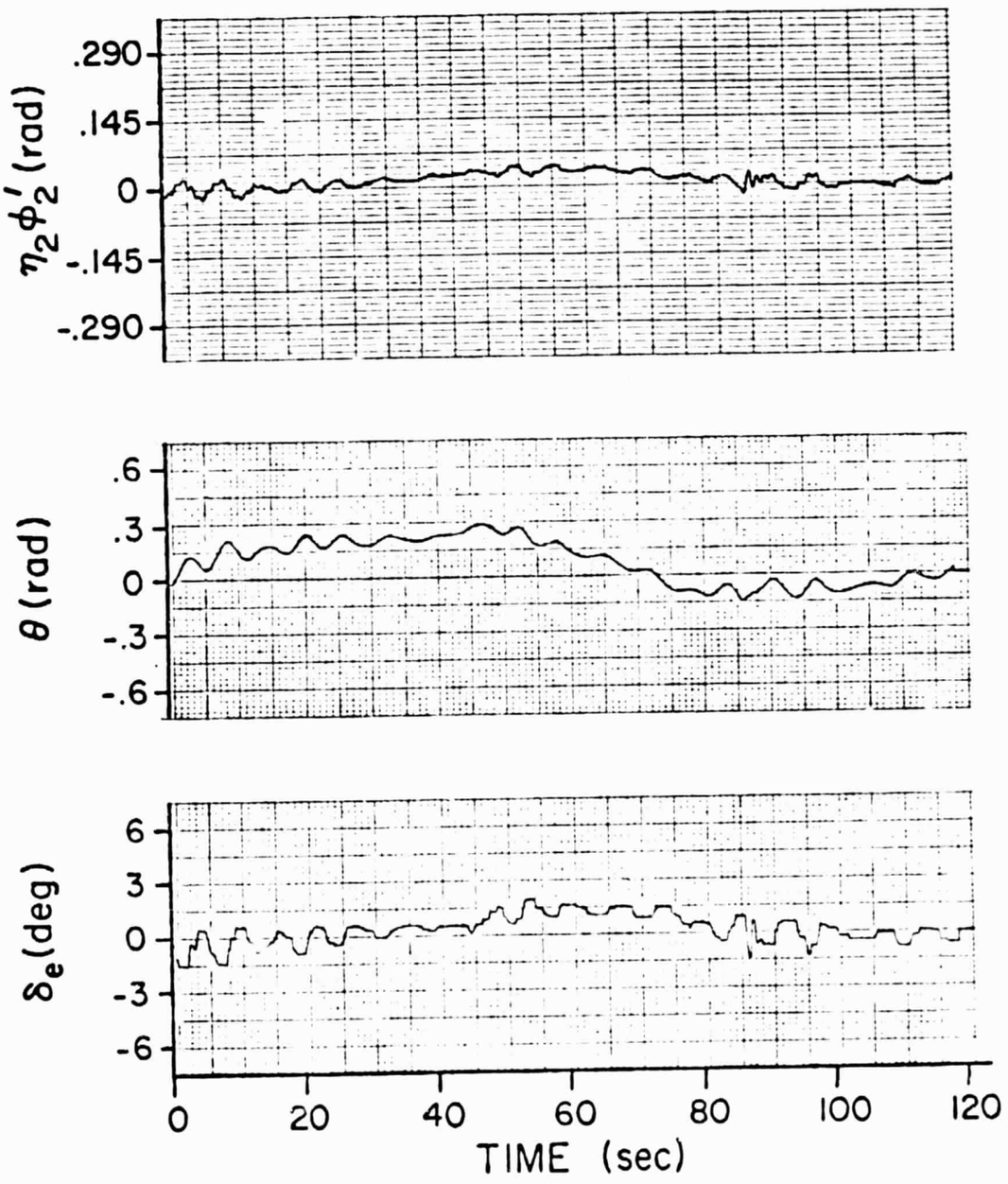

Figure 5.6B Sample Time History - Case 4

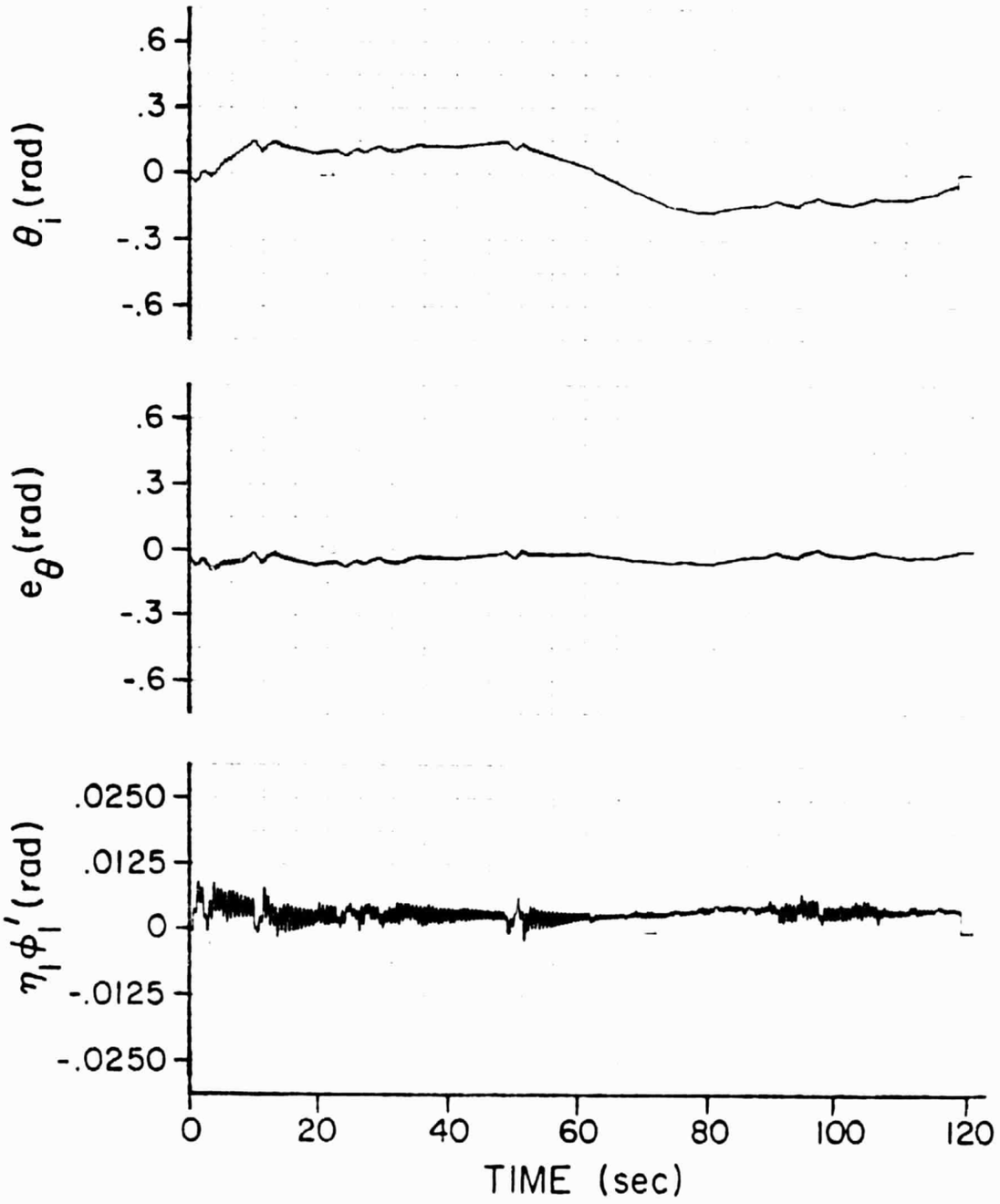

Figure 5.7A Sample Time History - Case 5

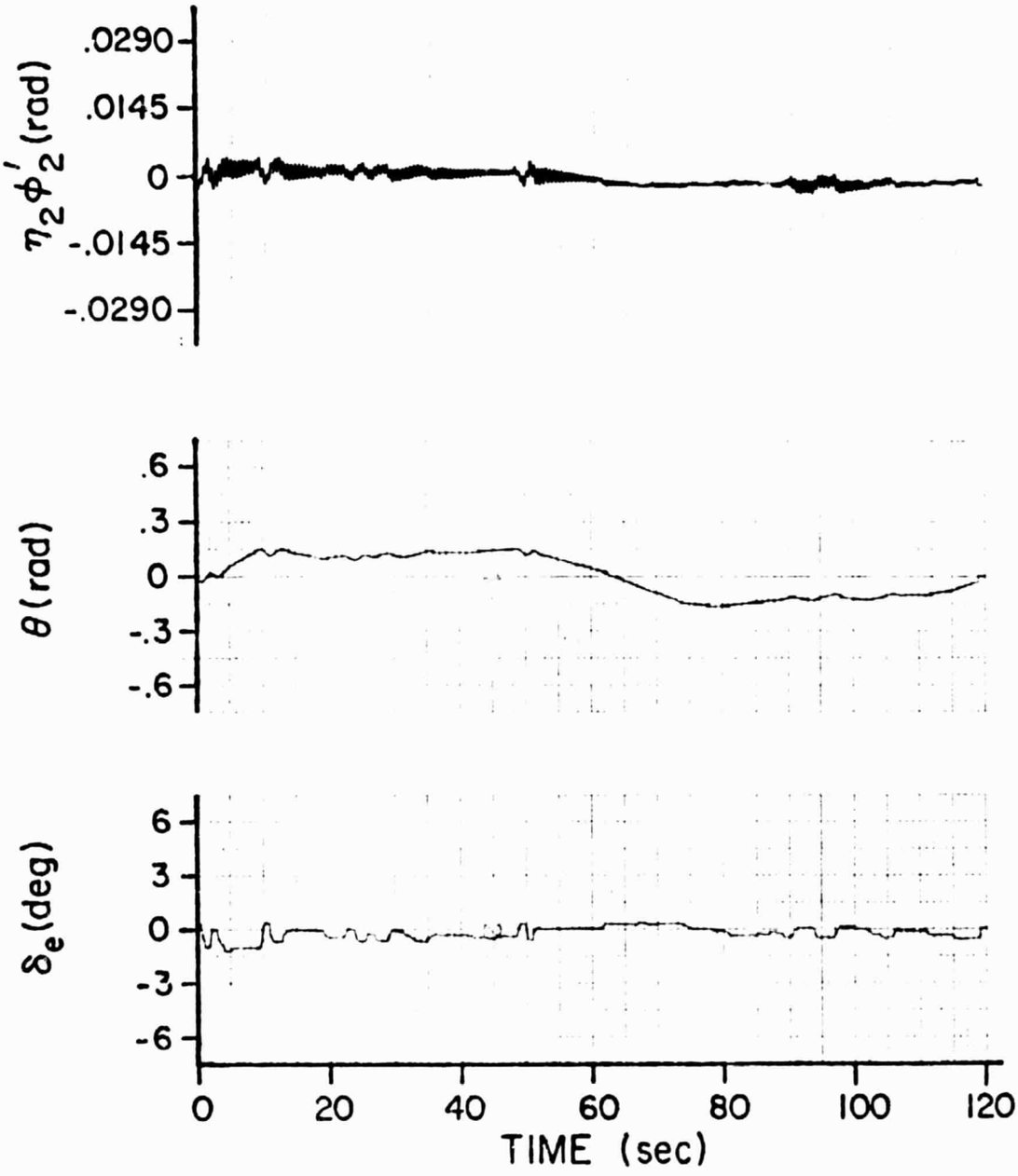

Figure 5.7B Sample Time History - Case 5

This oscillation causes annoyance to the pilot but is of no major concern due to its small magnitude.

Figures 5.8 is a sample time history plot for Case 6. In this case both $\eta_1\phi_1'$ and $\eta_2\phi_2'$ are much greater than that in Case 5, causing greater contribution to θ_i. θ_i is significantly increased. The pilot can not zero it out; e_θ is large. The difficulty in operating this case can be seen from the greater movement of the control stick (as shown by δ_e plot). Dynamic characteristics are the worst among the eight cases examined.

Figure 5.9 and Figure 5.10 are sample time histories for Case 7 and Case 8. $\eta_1\phi_1'$ and $\eta_2\phi_2'$ in Case 7 have greater contribution to θ_i than that in Case 8. The phenomena of oscillation in $\eta_1\phi_1'$ and $\eta_2\phi_2'$ is present in both cases. Elastic mode 2 is slightly unstable in Case 7, while it is stable in Case 8. However, in both cases, the pilot can operate the aircraft with ease; e_θ is small in both cases.

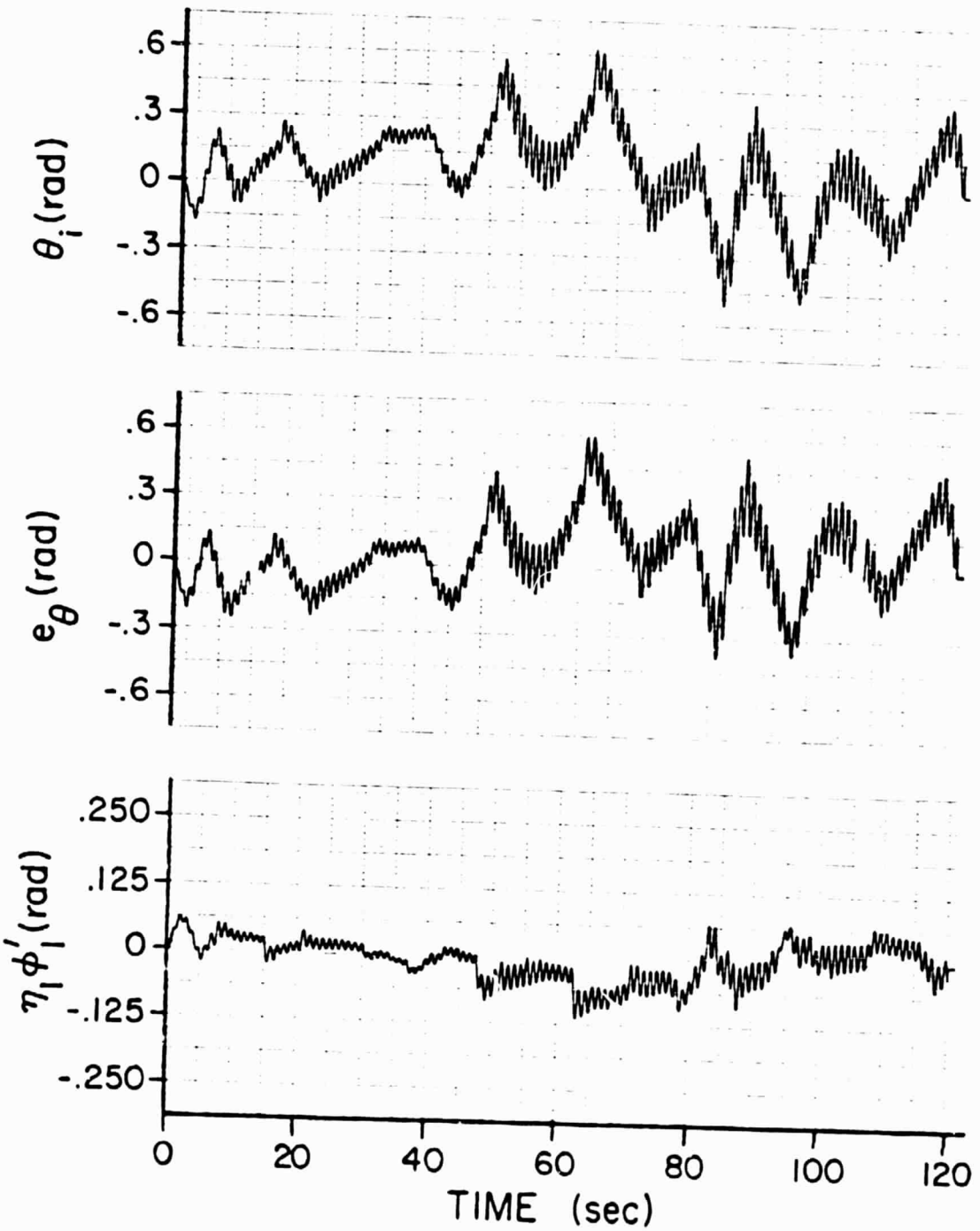

Figure 5.8A Sample Time History - Case 6

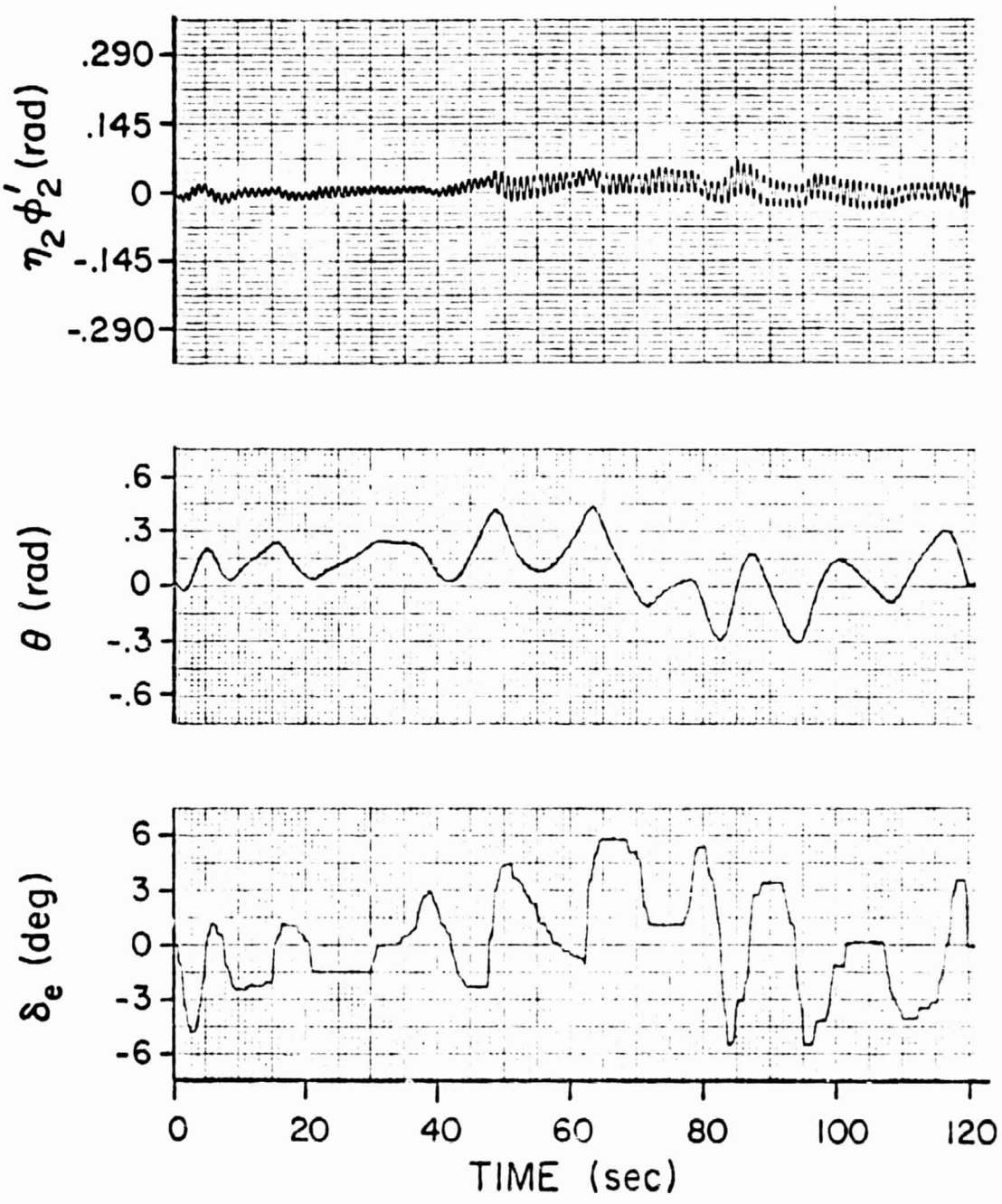

Figure 5.8B Sample Time History - Case 6

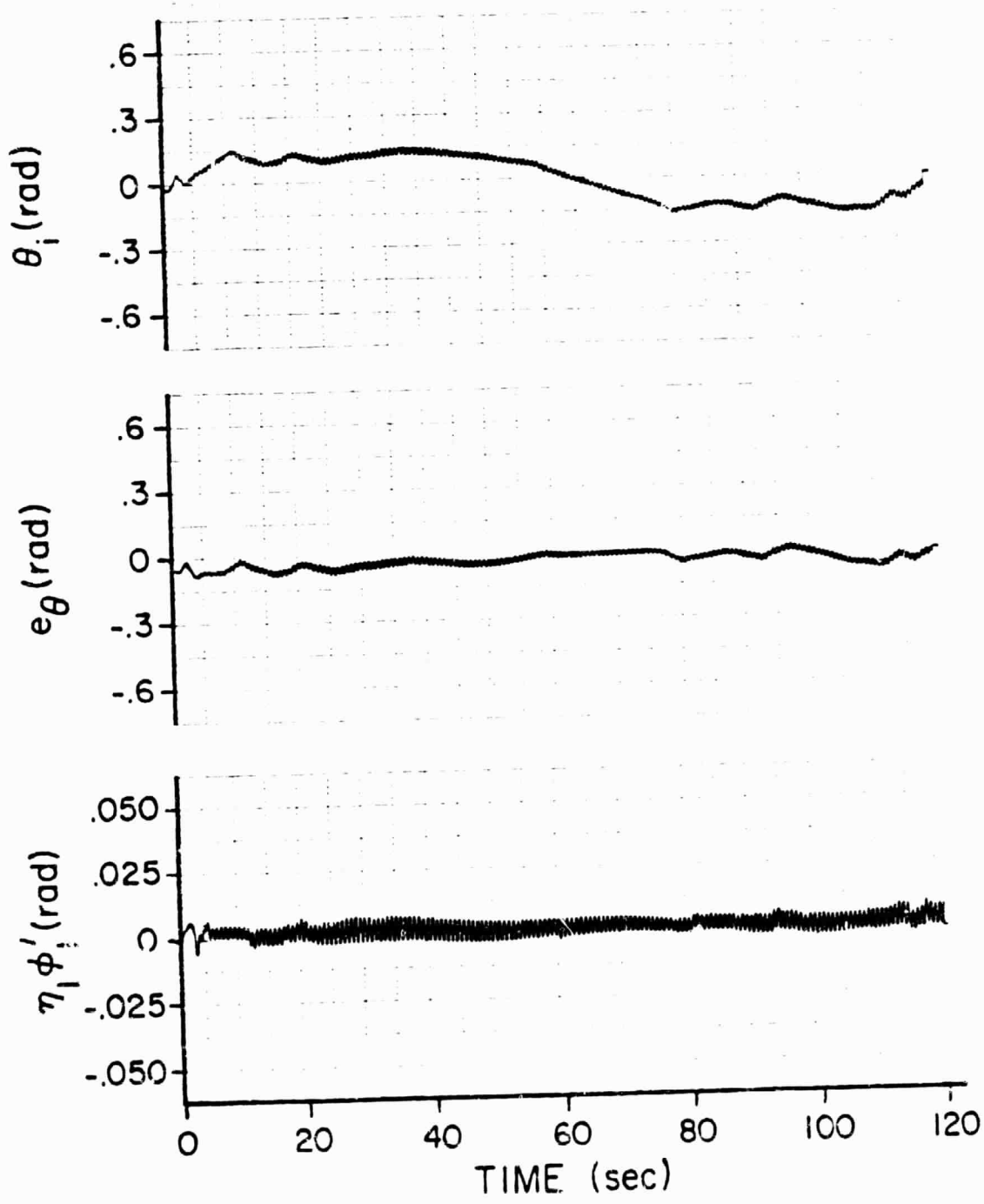

Figure 5.9A Sample Time History - Case 7

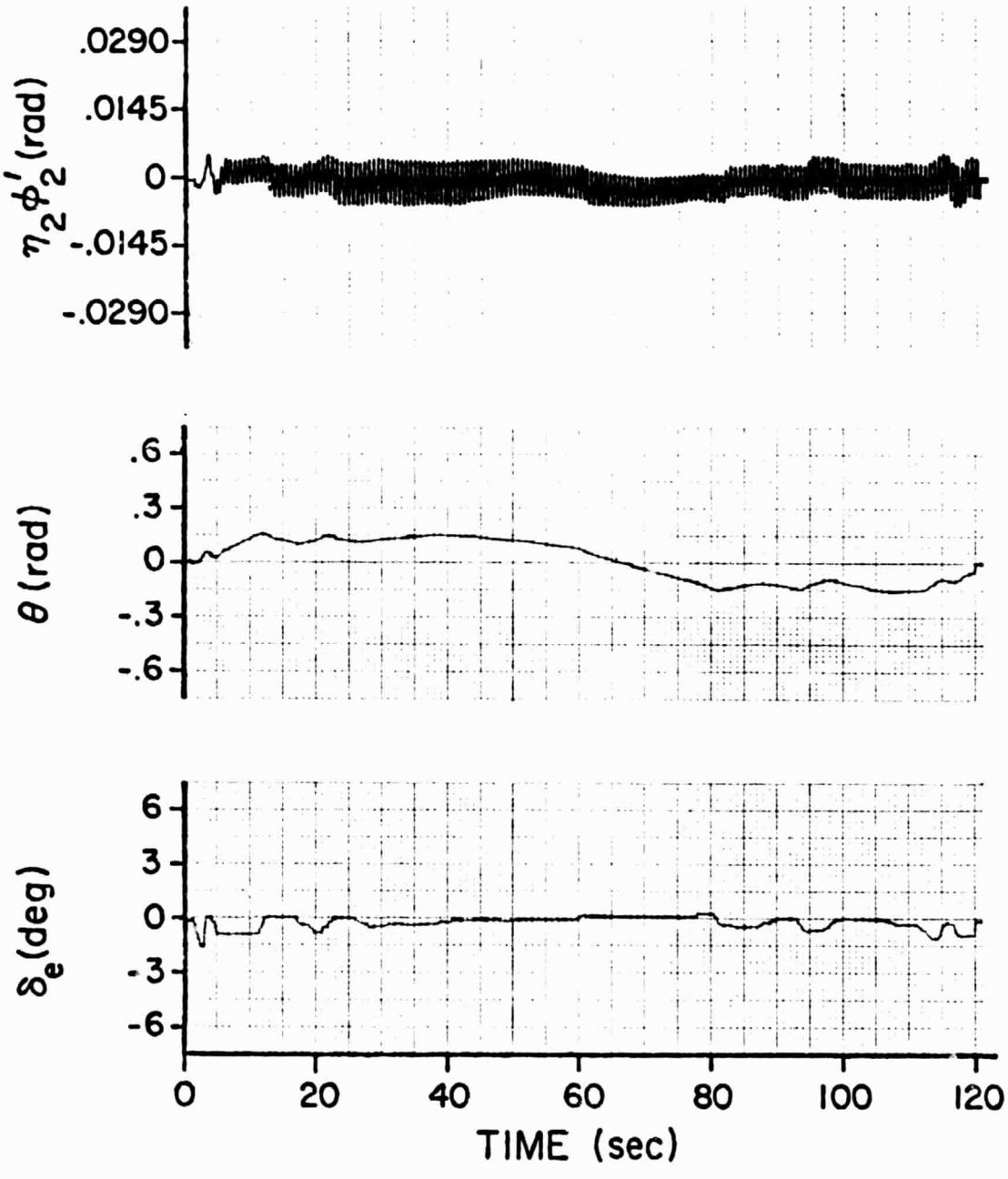

Figure 5.9B Sample Time History - Case 7

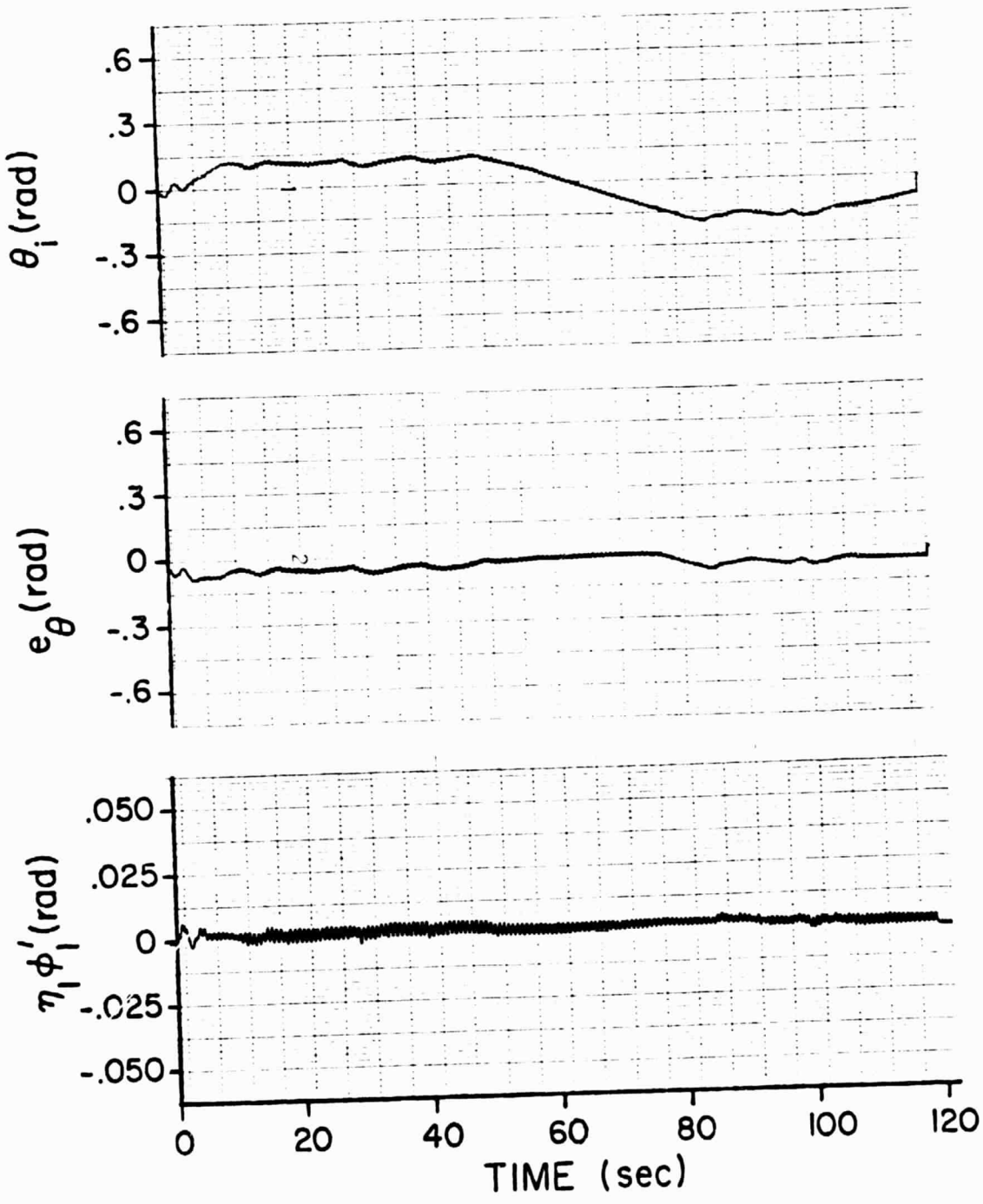

Figure 5.10A Sample Time History - Case 8

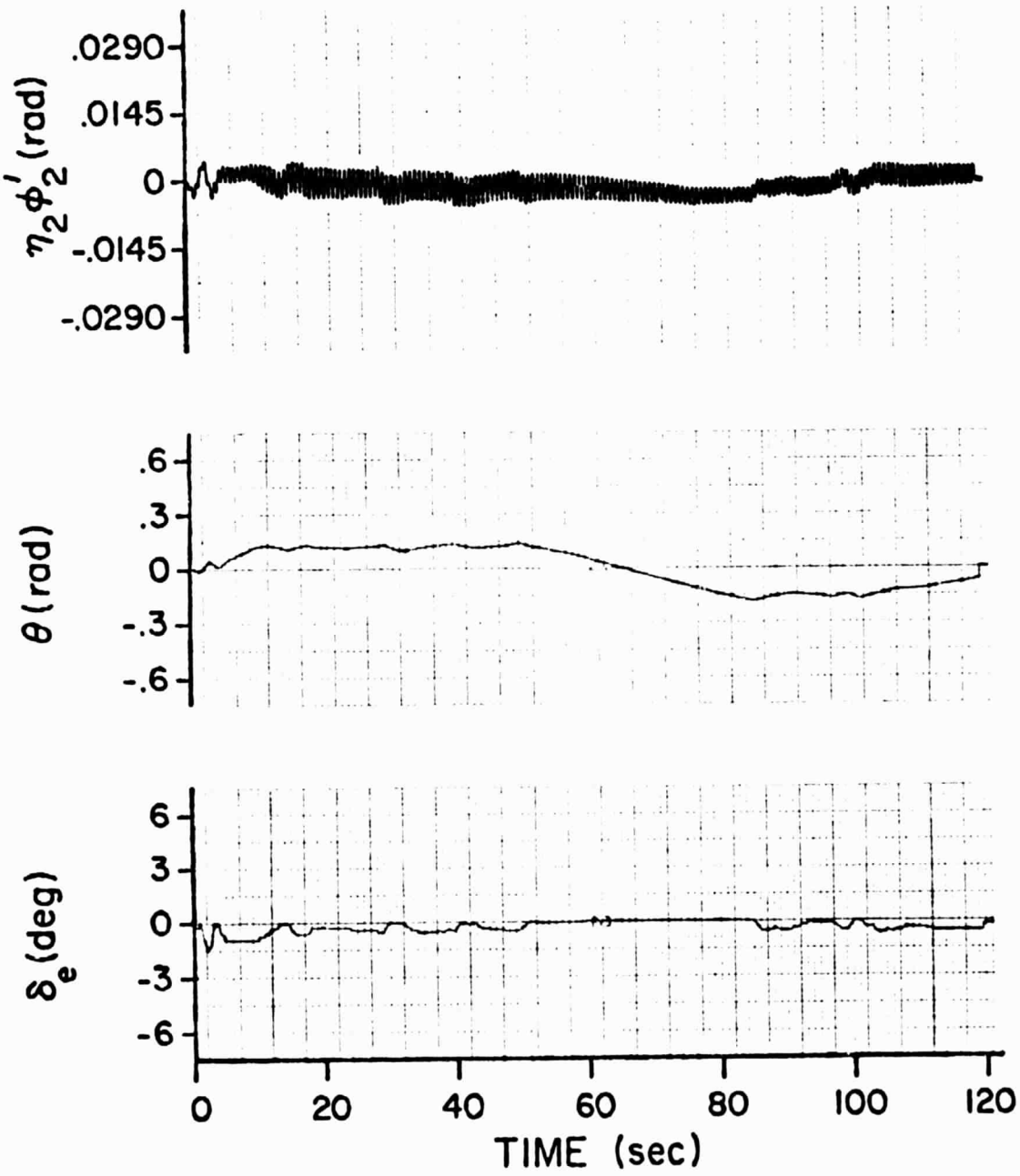

Figure 5.10B Sample Time History - Case 8

CHAPTER 6

SUMMARY, CONCLUSIONS, AND RECOMMENDATION

6.1 Summary

The longitudinal tracking task was evaluated using a fixed base simulation of the aircraft equations of motion. Pilots' comments on the task revealed the effect of low frequency dynamic aeroelasticity on the handling qualities and the pilot rating.

In Case 3 and Case 6 there is a large over shoot in the pitch angle error. These two cases received worse Cooper-Harper ratings indicating significant difficulty due to mode interaction. In Case 5, Case 7, and Case 8 there is not too much error in the pitch angle and the Cooper-Harper ratings are fair, but the pilots' comments are that it was annoying due to the oscillation from aeroelasticity. For the rest of the cases, the aeroelasticity has little effect on handling qualities and pilot ratings because of the minimal interaction with the rigid-body dynamics.

6.2 Conclusions

All conclusions are restricted to a constant altitude trim flight condition, which is the only flight condition which was investigated.

The most obvious conclusion is that the natural frequencies of elastic modes that were investigated represent good to very bad pilot ratings, primarily because of adverse aeroelastic mode interaction effects with rigid-body dynamics.

Elastic mode 1 affects handling qualities and pilot rating more than elastic mode 2 when the natural frequencies of the two elastic modes are reduced to the same numerical value.

From the point of view of handling qualities of rigid-body dynamics, Case 3 seems to have better handling qualities than Case 4. However, it is not true. So we have to look at $\eta_1\phi_1'$ and $\eta_2\phi_2'$ in pilot time history for Case 3 and Case 4, respectively. The θ_i was affected more in Case 3 than in Case 4 since $\eta_1\phi_1'$ contributes more to the value of θ_i in Case 3 than $\eta_2\phi_2'$ contributes to the value of θ_i in Case 4.

As seen in Case 7 and Case 8, the pilot rating is the same as the original case (Case 1). From the pilot time history and comments we know the small elastic oscillation can be visually separated from rigid-body

dynamics by the pilot. The elasticity is only slightly annoying to the pilot since the elastic modes do not significantly affect the rigid-body dynamics.

In Case 6 both natural frequencies of the two elastic modes were reduced to a still greater extent. This is the worst investigated and resulted in the poorest pilot ratings.

The results of the study indicate that handling qualities and pilot rating are functions of the natural frequencies of the elastic modes. The lower the value of natural frequency of an elastic mode, the worse the handling qualities and pilot ratings. This was due to adverse coupling effects on the phugoid dynamics and a larger contribution from the elastic mode amplitudes to the total pitch angle θ_i.

6.3 A Recommendation

In this study, the natural frequencies of the elastic modes were lowered from their nominal values to values close to the nominal short period frequency. However, this resulted in mode interaction which lowered the short period frequency and caused the phugoid mode to split into positive and negative real roots. Much of the pilots' difficulty in tracking on the worst cases was thus due to the positive phugoid root.

Table A.1 Normalization of Variables

Variable	Normalization
u	100 volts = 400 ft/sec
α	0.2 rad
θ	0.6 rad
$\dot{\theta}$	0.2 rad
θ_i	0.6 rad
η_1	10
$\dot{\eta}_1$	50
η_2	10
$\dot{\eta}_2$	50
h	6000 ft
δ_e	1.0 rad
δ_t	50,000 lbs

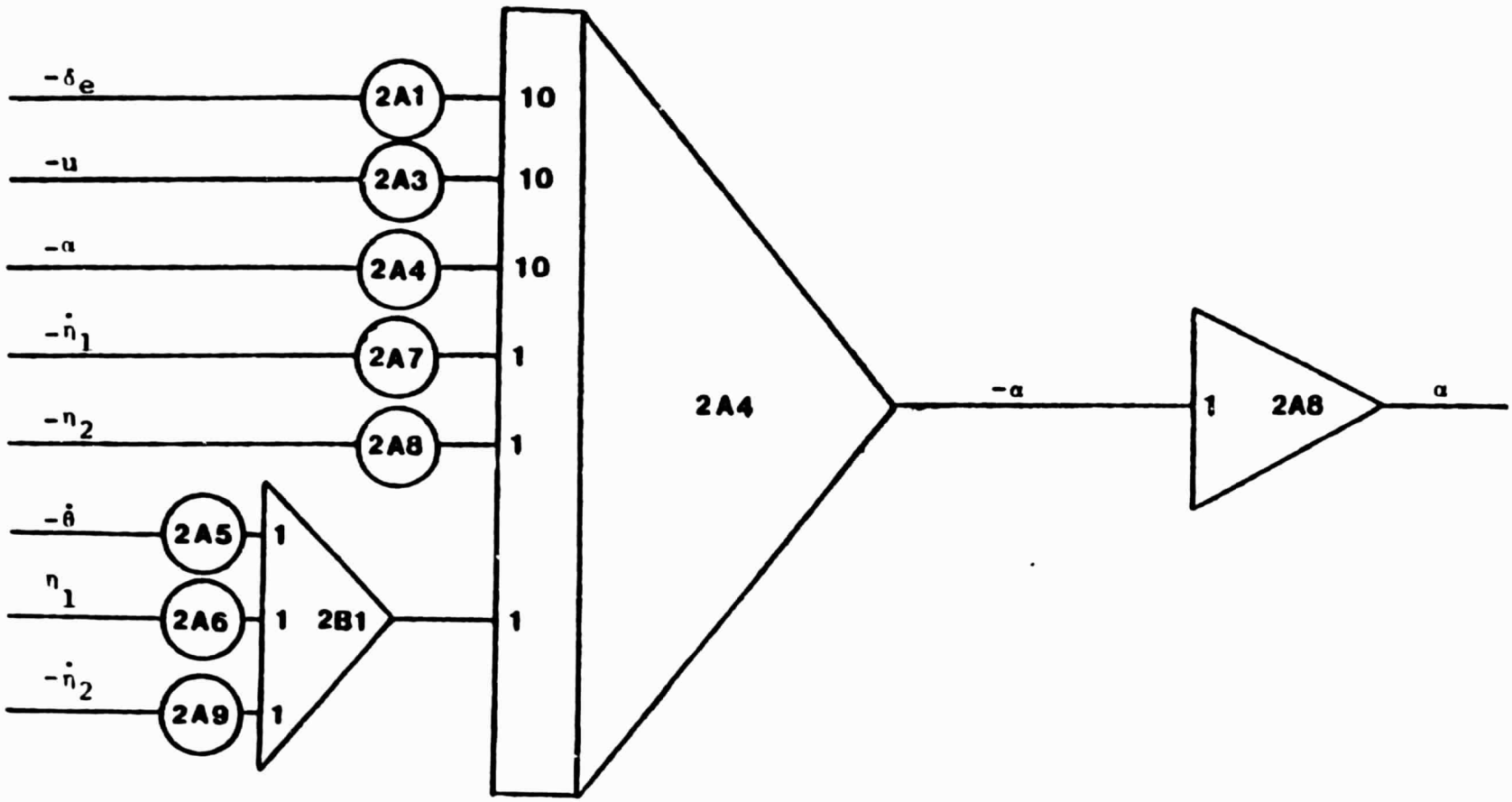

Figure A.1 Z-Force Equation

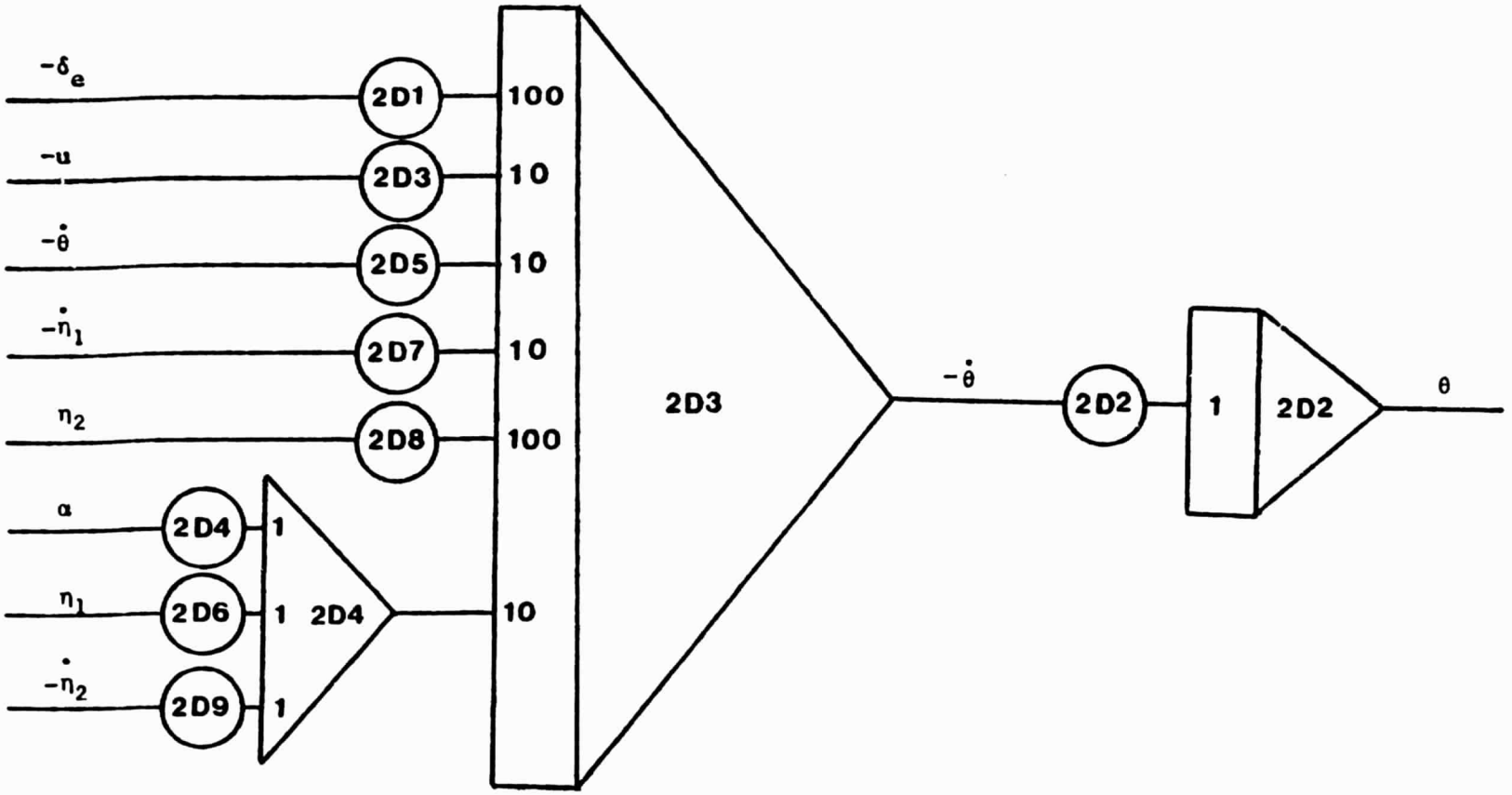

Figure A.2 Pitching Moment Equation

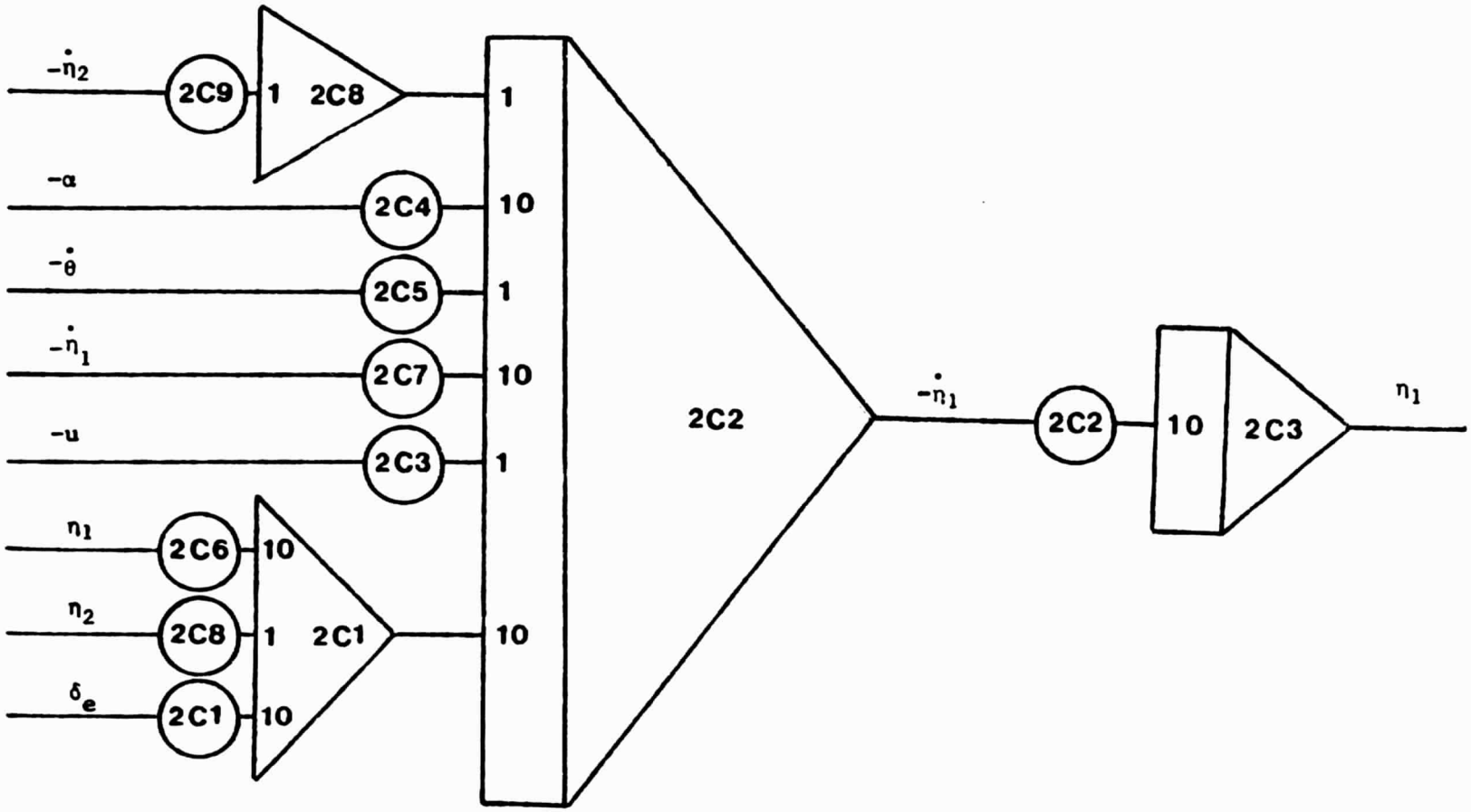

Figure A.3 Structural Mode 1 Equation

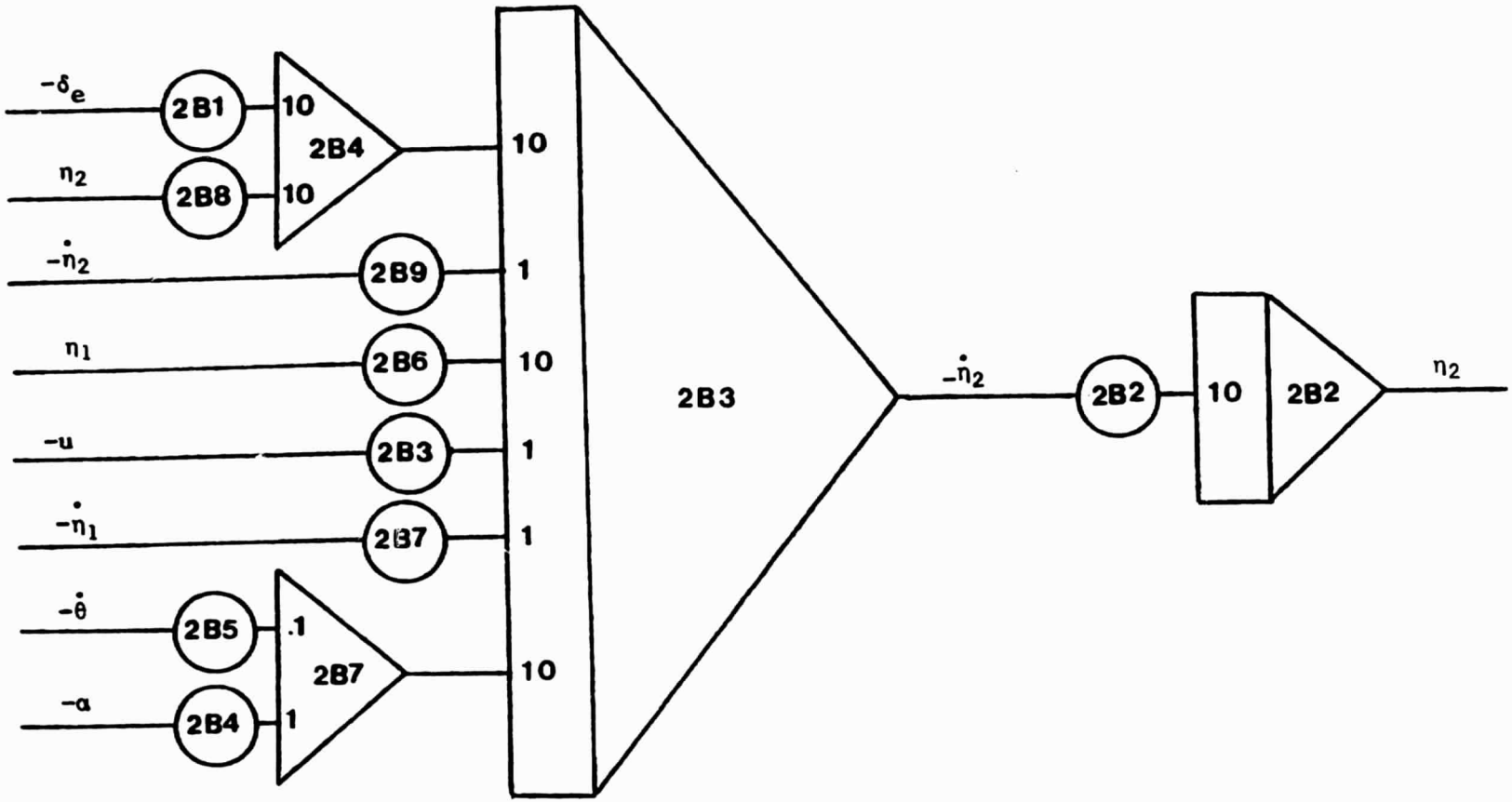

Figure A.4 Structural Mode 2 Equation

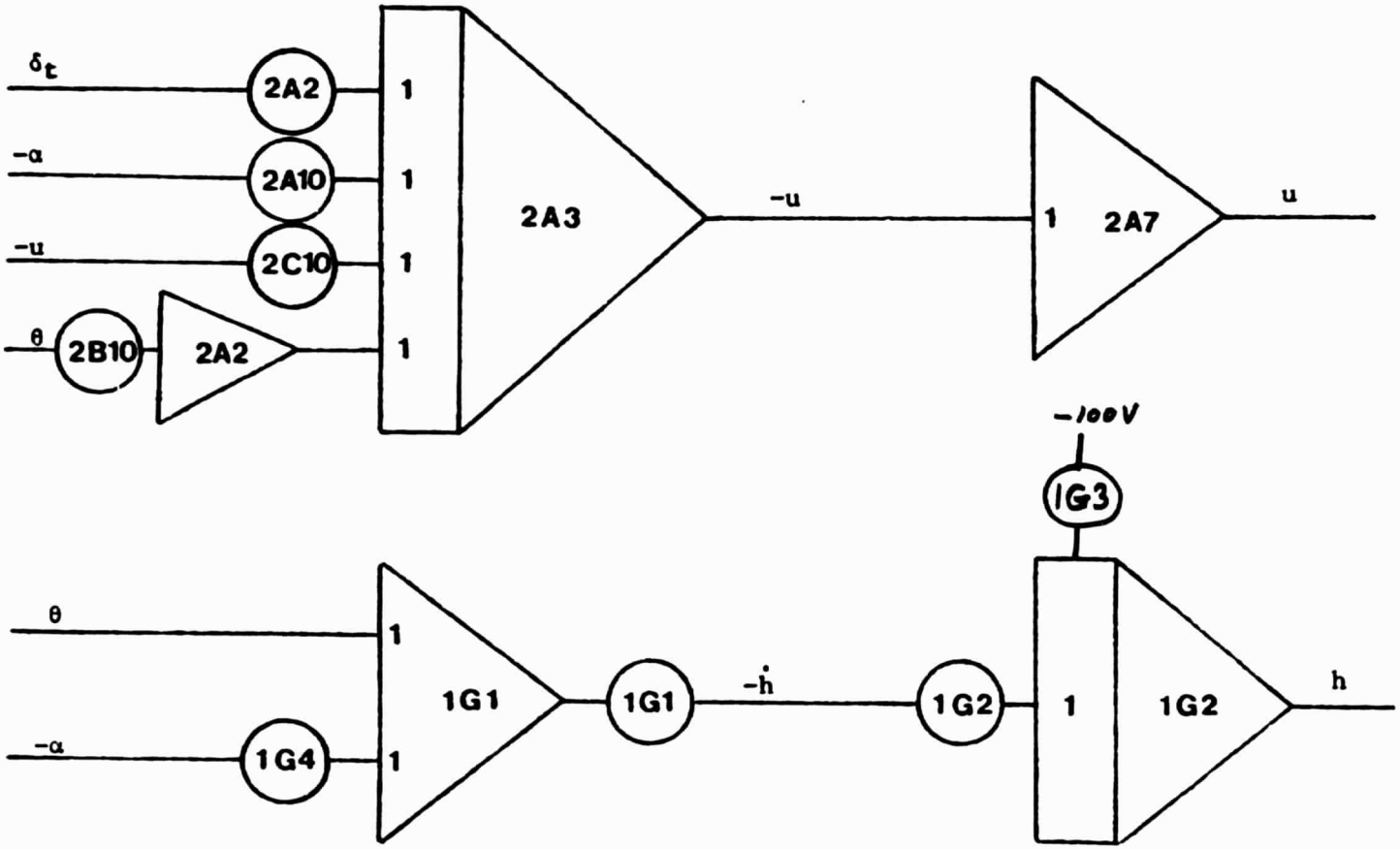

Figure A.5 X-Force Equation and Altitude Equation

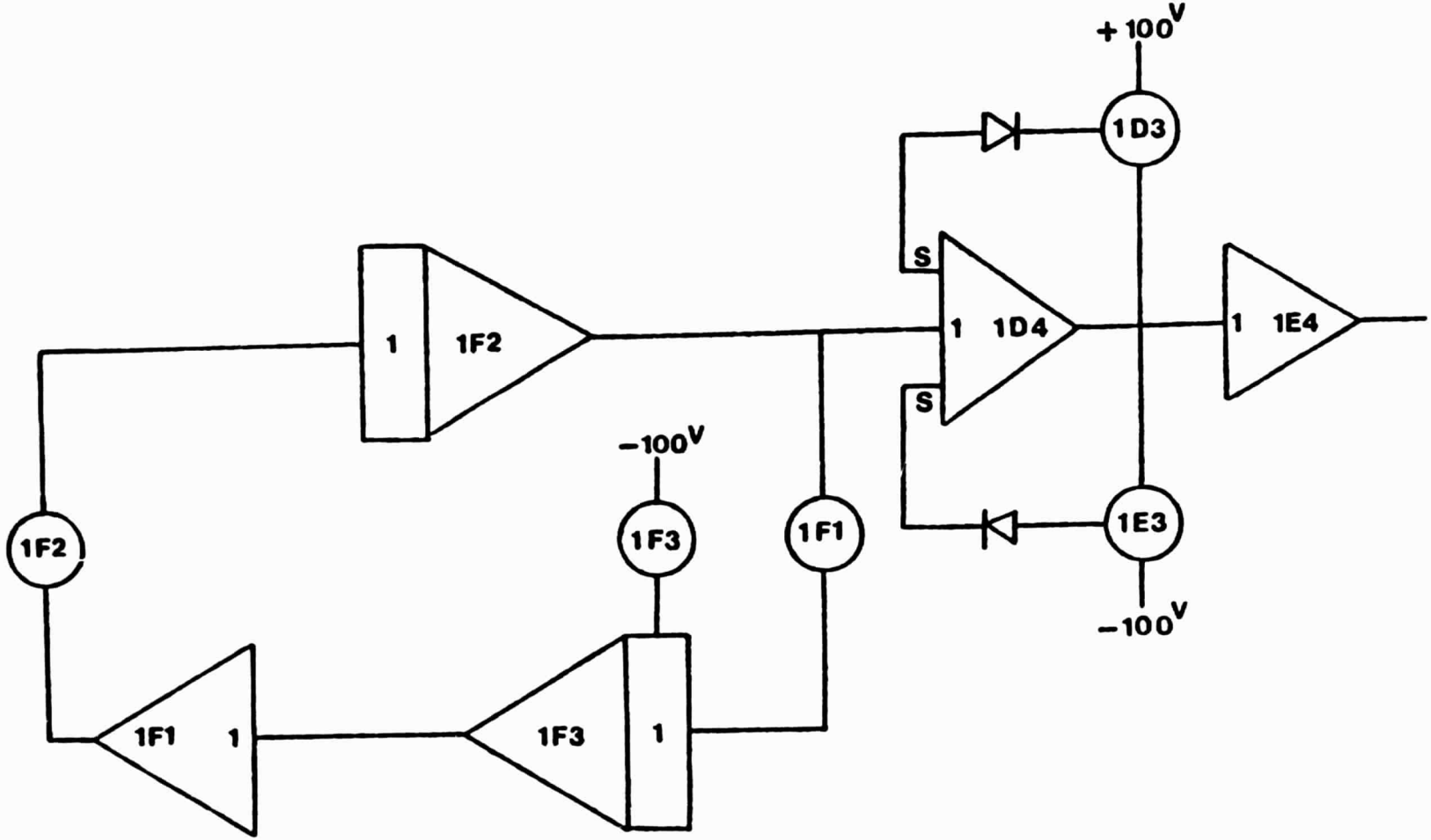

Figure A.6 Pitch Command Input

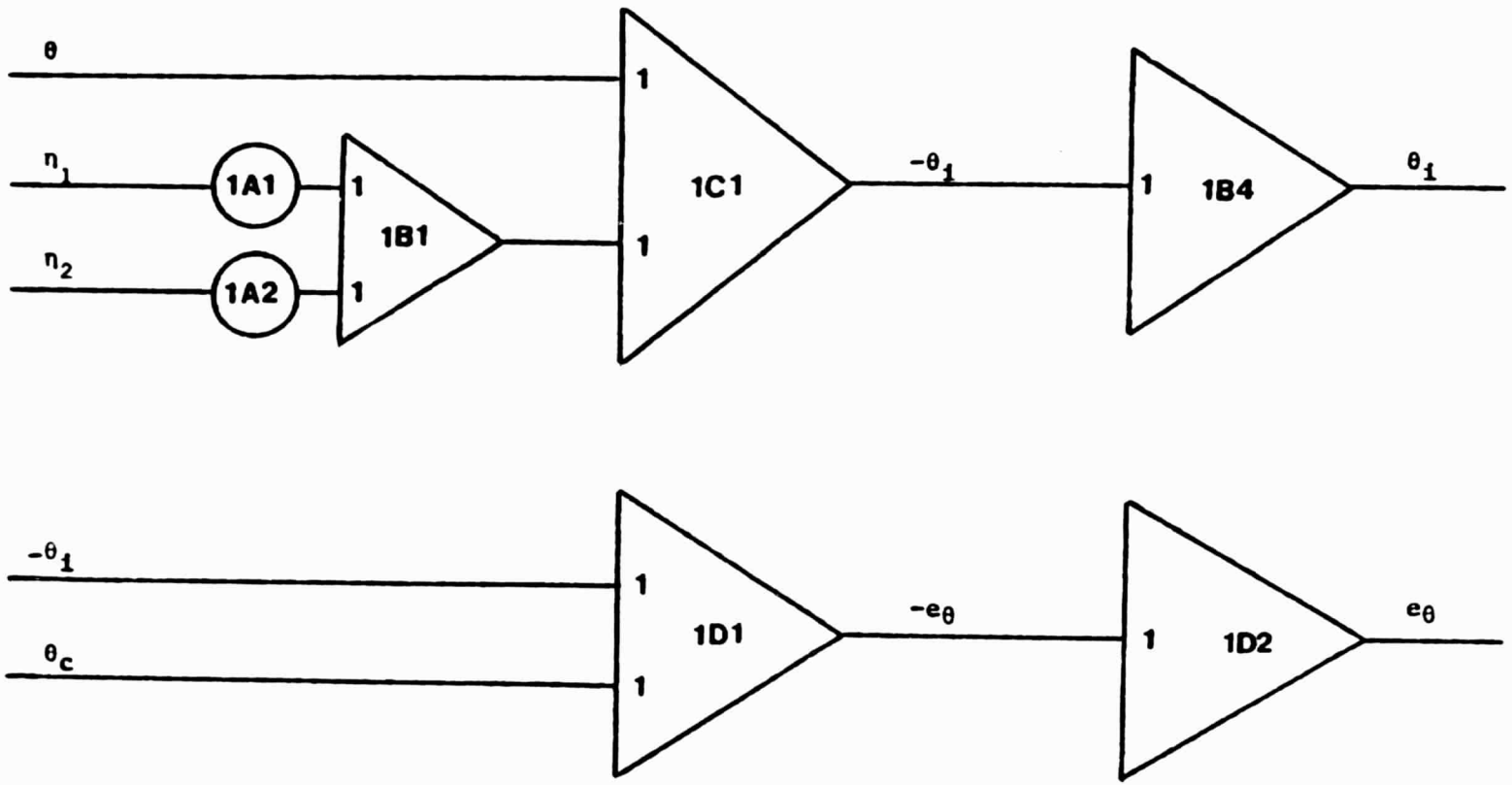

Figure A.7 Flight Director Equation and Pitch Angle Error Equation

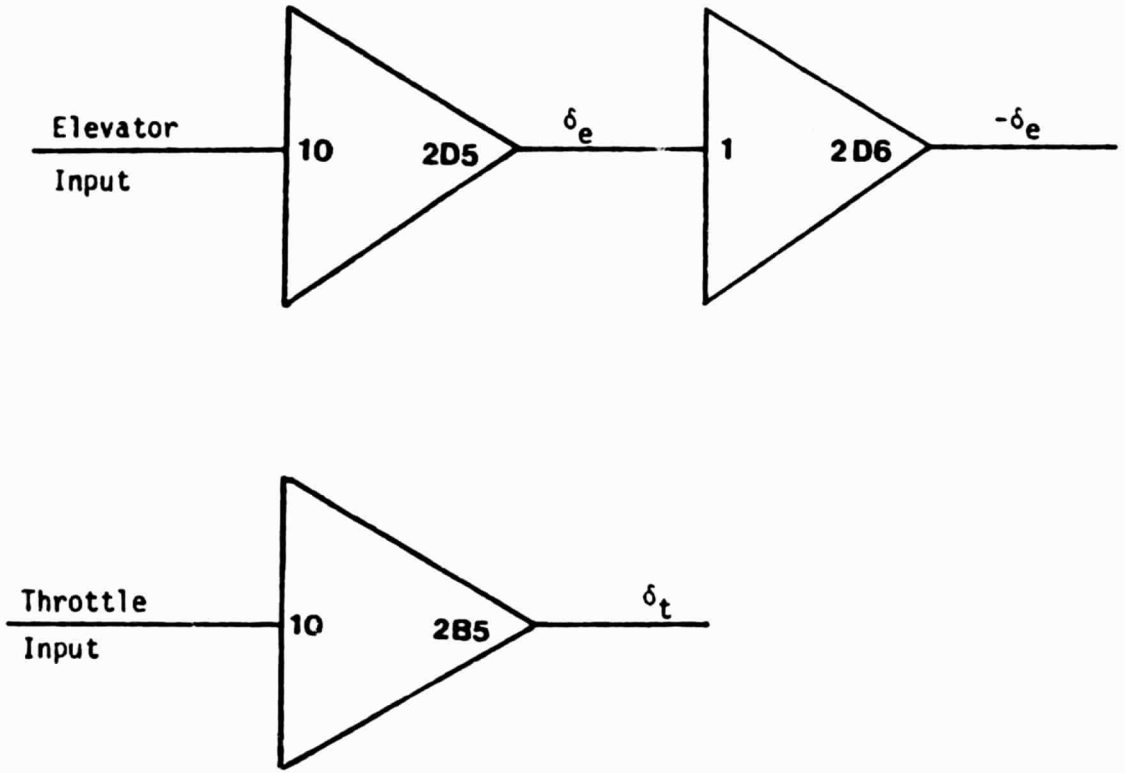

Figure A.8 Control Input

Table A.2 Potentiometer Settings

2A1	.144	2B1	.123
2A2	.029	2B2	.500
2A3	.130	2B3	.032
2A4	.121	2B4	.310
2A5	.943	2B5	.224
2A6	.453	2B6	.140
2A7	.053	2B7	.122
2A8	.233	2B8	.913
2A9	.038	2B9	.849
2A10	.013	2B10	.048
2C1	.446	2D1	.753
2C2	.500	2D2	.333
2C3	.012	2D3	.456
2C4	.295	2D4	.707
2C5	.533	2D5	.202
2C6	.355	2D6	.923
2C7	.114	2D7	.186
2C8	.308	2D8	.104
2C9	.915	2D9	.174
2C10	.025		
1A1	.625	1F1	.052
1A2	.725	1F2	.052

Table A.2, cont.

1G1	.333	1F3	.600
1G2	.094	1D3	.200
1G3	.750	1E3	.200
1G4	.333		

Table 2.3 Potentiometer Settings for Eight Cases

Case 1:		Case 5:	
2C6	.355	2C6	.258
2C7	.114	2C7	.110
2B8	.913	2B8	.288
2B9	.849	2B9	.658
Case 2:		**Case 6:**	
2C6	.154	2C6	.082
2C7	.105	2C7	.101
2B8	.913	2C8	.112
2B9	.849	2C9	.564
Case 3:		**Case 7:**	
2C6	.062	2C6	.196
2C7	.099	2C7	.107
2B8	.913	2B8	.206
2B9	.849	2B9	.620
Case 4:		**Case 8:**	
2C6	.355	2C6	.214
2C7	.114	2C7	.108
2B8	.062	2B8	.188
2B9	.521	2B9	.611